

Calibration of a mechanism-based method against NLFEA for NLPO analyses of URM terraced house units

Cross-validation and calibration of simplified methods for different building typologies

Messali, F.; Longo, M.

Publication date

2019

Document Version

Final published version

Citation (APA)

Messali, F., & Longo, M. (2019). *Calibration of a mechanism-based method against NLFEA for NLPO analyses of URM terraced house units: Cross-validation and calibration of simplified methods for different building typologies*. Delft University of Technology.

Important note

To cite this publication, please use the final published version (if applicable). Please check the document version above.

Copyright

Other than for strictly personal use, it is not permitted to download, forward or distribute the text or part of it, without the consent of the author(s) and/or copyright holder(s), unless the work is under an open content license such as Creative Commons.

Takedown policy

Please contact us and provide details if you believe this document breaches copyrights. We will remove access to the work immediately and investigate your claim.

<i>Project number</i>	TC19/20
<i>File reference</i>	TC19/20-R01
<i>Date</i>	6 December 2019
<i>Corresponding author</i>	Francesco Messali (f.messali@tudelft.nl)

Cross-validation and calibration of simplified methods for different building typologies

CALIBRATION OF A MECHANISM-BASED METHOD AGAINST NLFEA FOR NLPO ANALYSES OF URM TERRACED HOUSE UNITS

Authors: Francesco Messali, Michele Longo


Cite as: *Messali, F., Longo, M. Calibration of a mechanism-based method against NLFEA for NLPO analyses of URM terraced house units. Report no. TC19/20-R01, Version 01, 6 December 2019. Delft University of Technology*

This document is made available via the website 'Structural Response to Earthquakes' and the TU Delft repository. While citing, please verify if there are recent updates of this research in the form of scientific papers.

All rights reserved. No part of this publication may be reproduced, stored in a retrieval system of any nature, or transmitted, in any form or by any means, electronic, mechanical, photocopying, recording or otherwise, without the prior written permission of TU Delft.

TU Delft and those who have contributed to this publication did exercise the greatest care in putting together this publication. This report will be available as-is, and TU Delft makes no representations of warranties of any kind concerning this Report. This includes, without limitation, fitness for a particular purpose, non-infringement, absence of latent or other defects, accuracy, or the presence or absence of errors, whether or not discoverable. Except to the extent required by applicable law, in no event will TU Delft be liable for on any legal theory for any special, incidental consequential, punitive or exemplary damages arising out of the use of this report.

This research work was funded by y Stichting Koninklijk Nederlands Normalisatie Instituut (NEN) under project number 8505400024-001.

 <p> Faculty of Civil Engineering and Geosciences Stevinweg 1 2628 CN Delft PO 5048 2600 GA Delft www.citg.tudelft.nl </p>		REPORT	
		<i>Title:</i> Calibration of a mechanism-based method against NLFEA for NLPO analyses of URM terraced house units	
		<i>Author(s):</i> Francesco Messali Michele Longo	
		<i>Date:</i> 06/12/2019	
<i>Client(s):</i> Nationaal Coördinator Groningen (NCG)		<i>Version:</i> 01	<i>Status:</i> Final
<i>Project number:</i> TC19/20	<i>Project name:</i> Cross-validation and calibration of simplified methods for different building typologies		<i>File reference:</i> TC19/20-R01
<i>Cite as:</i> Messali, F., Longo, M. Calibration of a mechanism-based method against NLFEA for NLPO analyses of URM terraced house units. Report no. TC19/20-R01, Version 01, 6 December 2019. Delft University of Technology			

Copyright statement

All rights reserved. No part of this publication may be reproduced, stored in a retrieval system of any nature, or transmitted, in any form or by any means, electronic, mechanical, photocopying, recording or otherwise, without the prior written permission of TU Delft.

Liability statement

TU Delft and those who have contributed to this publication did exercise the greatest care in putting together this publication. However, the possibility should not be excluded that it contains errors and imperfections. Any use of this publication and data from it is entirely on the own responsibility of the user. For everybody who has contributed to this publication, TU Delft disclaims any liability for damage that could result from the use of this publication and data from it, unless the damage results from malice or gross negligence on the part of TU Delft and/or those who have contributed to this publication.

Executive summary

Introduction

This document presents a numerical study that aims to calibrate simplified models (mechanism-based analyses) against more sophisticated nonlinear finite element analyses (NLFEA) for unreinforced masonry (URM) terraced houses. The comparison between the analyses focuses on the parameters of the equivalent bilinear capacity curve, especially on: (i) the initial stiffness K_{ini} ; (ii) the base shear capacity V_u ; (iii) the displacement capacity d_{vc} . For each parameter, possible correction factors are identified. These factors can be applied to align the results of the simplified methods with those obtained via sophisticated NLFEA.

The mechanism-based analyses are performed according to the SLaMA method as described in NPR 9998 [1], while the NLFEA are also NPR-based and are run with the software DIANA FEA 10.3.

Analyses performed

The experimentally tested full-scale building EUC-BUILD-6, tested on a shake table at the laboratory of EUCENTRE (Pavia, Italy), was taken as a reference building for a terraced house unit. The NLFEA model was originally calibrated against the experimental test in a previous study carried out by TU Delft [2]. To consider the variability of the terraced houses, analyses of structures with variations of the following characteristics have been considered:

- Layout of the façades, including variations of the opening percentage;
- Masonry type, including a variation of the connection at corners between transversal walls;
- Number of storeys and floor type at attic level;
- Connection between the floor and the loadbearing façade.

In total 48 3D FEM and SLaMA analyses of the complete building and 1040 2D FEM and SLaMA analyses of a single façade have been performed. As an example, Figure A shows the bilinearized curves obtained from the 48 3D NLFEA and SLaMA analyse. The thicker and darker lines highlight the average curves.

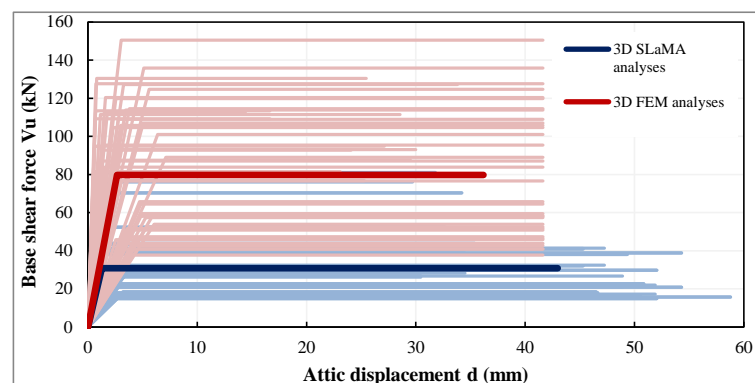


Figure A. Bilinearized curves obtained from the 48 3D NLFEA computations and SLaMA analyses (the average curves are thicker and darker).

Conclusions

The conclusions are mainly based on the results of the 3D analyses, while the 2D analyses are used to identify the influence of each variation on the capacity curves.

The analyses performed lead to the following conclusions:

1. The failure mechanism is usually governed by rocking of the piers at the ground storey. For the 3D analyses, a governing rocking mechanism was predicted by both NLFEA and SLaMA for 85% of the

- cases. In 9% both predicted a shear failure mechanism. In the remaining cases no clear governing mechanism could be identified in the NLFEA while SLaMA predicted flexural (rocking) failure.
- The initial stiffness K_m derived by the NLFEA is on average a factor 1.24 larger than the stiffness computed with the SLaMA method.
 - The near collapse displacement capacity d_{NC} derived by the NLFEA is on average a factor 0.85 smaller than the stiffness computed with the SLaMA method.
 - The NPR-based global drift limit at inter-storey level applied to the NLFEA for ductile mechanisms (1.5%) differs by only 5% from the average near collapse displacement computed for the SLaMA analyses, which is mainly governed by the flexural displacement capacity of the single piers.
 - When the 3D analyses are considered, the NLFEA return a base shear capacity that is on average more than 2.5 times higher than that computed according to the SLaMA method, and on average 1.5 times higher for more than the 95% of the cases analysed.
 - For the following three cases the difference between the ultimate base shear computed with NLFEA and SLaMA is larger than for the other cases. Specifically, the ratio between the base shear computed according to NLFEA and SLaMA is always larger than 2.25 for the 12 corresponding 3D analyses: (a) buildings with CS elements; (b) cases when the loadbearing façade is not structurally connected to the RC floor at the first floor level; (c) cases when long, squat piers are present in the façade. This latter often determines other failure mechanisms (shear sliding, or diagonal cracking) than flexure.

Final recommendations for analyses of a terraced house unit

With regard to the initial stiffness and the ultimate displacement capacity of the building, no correction factor is suggested to be applied to SLaMA analyses (i.e. a factor equal to 1).

A correction factor can be applied to increase the value of the ultimate base shear computed with the SLaMA method:

- A correction factor 1.5 can be taken for a generic terraced house unit, because this provides conservative results with respect to the corresponding NLFEA in 95% of the cases analysed with 3D analyses (Figure B(a)).
- The correction factor can be increased up to the value 2 when a building presents one of the three following characteristics: (i) use of CS elements, (ii) structural continuity of the loadbearing façade (i.e. the RC floor is not connected to the inner leaf of the façade, except for anchors that will prevent the out-of-plane failure), (iii) presence of long, squat piers with an aspect ratio larger than one. The suggested value 2 is smaller than the minimum ratio between the base shear computed according to NLFEA and SLaMA for the twelve 3D simulations performed on buildings with such characteristics (as shown in Figure B(b), where the 12 simulations are highlighted by red markers).

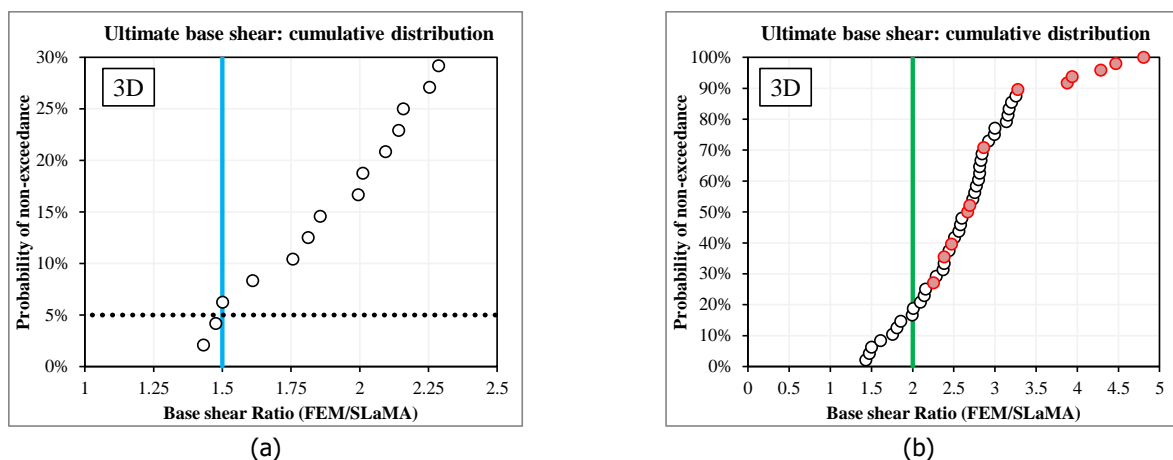


Figure B. Cumulative distribution functions for the ratio between the ultimate base shear computed for the results of 3D NLFEA and SLaMA analyses: detail for low probability of non-exceedance (a), and for the analyses with CS elements, structural continuity of the loadbearing façade and long piers, highlighted by red markers (b).

Table of Contents

Executive summary	3
1 Introduction	6
2 Reference building.....	7
3 Set of variations used for the validation study	8
3.1 Complete building.....	8
3.2 Single façade	10
4 Methodology used for SLaMA and NLFEA	12
4.1 SLaMA models.....	12
4.2 Finite Element models in Diana 10.3	14
5 Comparison of the results	16
5.1 3D analyses	16
5.2 2D analyses	21
6 Conclusions.....	28
References.....	30

1 Introduction

The work described in the current document is part of the project “Cross-validation and calibration of simplified methods for different building typologies”, which aims at the calibration of simplified models against more sophisticated nonlinear finite element analyses (NLFEA) for specific building typologies. Namely, the project focuses on the calibration of the mechanism-based analyses (SLaMA method) against full NLFEA for nonlinear pushover (NLPO) analyses. This work follows up the preliminary investigation performed by TU Delft and presented to NEN in September 2018 [1] on a comparison between the peak base shear capacity of seven full-scale URM buildings computed according to different computational methods.

In the proposal document of the project [4], three specific building groups are identified: (i) terraced and semi-detached houses; (ii) detached houses; (iii) farmhouses. The work described in this document is limited to the first building group, and particularly to terraced houses. This group of buildings is characterized by a resisting system composed of unreinforced masonry (URM) walls, large openings and vertical irregularities on the façades and solid walls in the transversal direction, cavity walls with calcium silicate (CS) masonry commonly used for the loadbearing walls, one or two storeys up to the attic level. This buildings belongs to clusters 2B/F according to the categorization presented by CVW [5][6].

The proposal document identifies building EUC-BUILD-6, which was tested in dynamic conditions on a shake table at the laboratory of EUCENTRE (Pavia, Italy), as a reference building for this group of buildings. A short description of building EUC-BUILD-6 is provided in Section 2, and more details are available in the original testing report [7]. The comparison between the different analyses focuses on the equivalent bilinear curve, and especially on the following parameters: (i) the initial stiffness K_{in} ; (ii) the base shear capacity V_b ; (iii) the displacement capacity d_{NC} . The present work aims eventually to identify and recommend possible correction (“model”) factors that, when applied to the results of the simplified methods, may allow to get results in line with those obtained via more sophisticated NLFEA.

Since a single analysis is not enough to compare the results obtained with simplified and sophisticated approaches, an extensive sensitivity study is carried out to complement the research. The sensitivity study is based on the following key parameters:

- Building regularity (layout of the façades), including variations of the opening percentage;
- Masonry type, including a variation of the connection at corners between transversal walls;
- Number of storeys and floor type at attic level;
- Connection between the floor and the loadbearing façade.

In addition, different lateral load distributions and loading directions are considered.

Along with the analysis of the complete building, also 2D analyses of a single façade are performed in order to investigate the origin of the differences in terms of structural in-plane capacity between the results obtained with simplified and sophisticated analyses. A description of all the variations is provided in Section 3. More details can be found in the plan of approach [8].

The methodology followed to simulate the structural behaviour with the NLFEA and the SLaMA method is summarised in Section 4. A comparison between the results obtained with the two analyses is presented in Section 5. The conclusive remarks with the proposal of the model factors can be found in Section 6.

2 Reference building

As mentioned in Section 1, the building EUC-BUILD-6 is taken as reference building for the current study. This building was tested dynamically on a shake table at the laboratory of EUCENTRE (Pavia, Italy) in 2018. EUC-BUILD-6 refers to a two-storey URM cavity-wall terraced house of the late 1970s, characterised by large openings at the ground floor of the front façade. The building is made of cavity-walls with the load-bearing inner leaf made of CS bricks and a veneer made of clay bricks. The first floor is a rigid diaphragm built with precast reinforced concrete panels and a structural topping slab, while the second-floor and the roof are flexible diaphragms made of timber joists and planks. The floor systems are often discontinuous between adjacent units and rest only on transverse CS walls [7], with the intermediate transverse walls made of two independent CS leaves. Because of this, each unit is structurally separated from those adjacent (only the veneers are structurally continue) and EUC-BUILD-6 is then representative of the end-unit of the terraced house (Figure 1).

A complete description of EUC-BUILD-6 is provided in the testing report [7].



Figure 1. Front façade of the terraced house considered as reference building. The end unit represented by EUC-BUILD -6 is highlighted in the picture (picture from the testing report [7]).

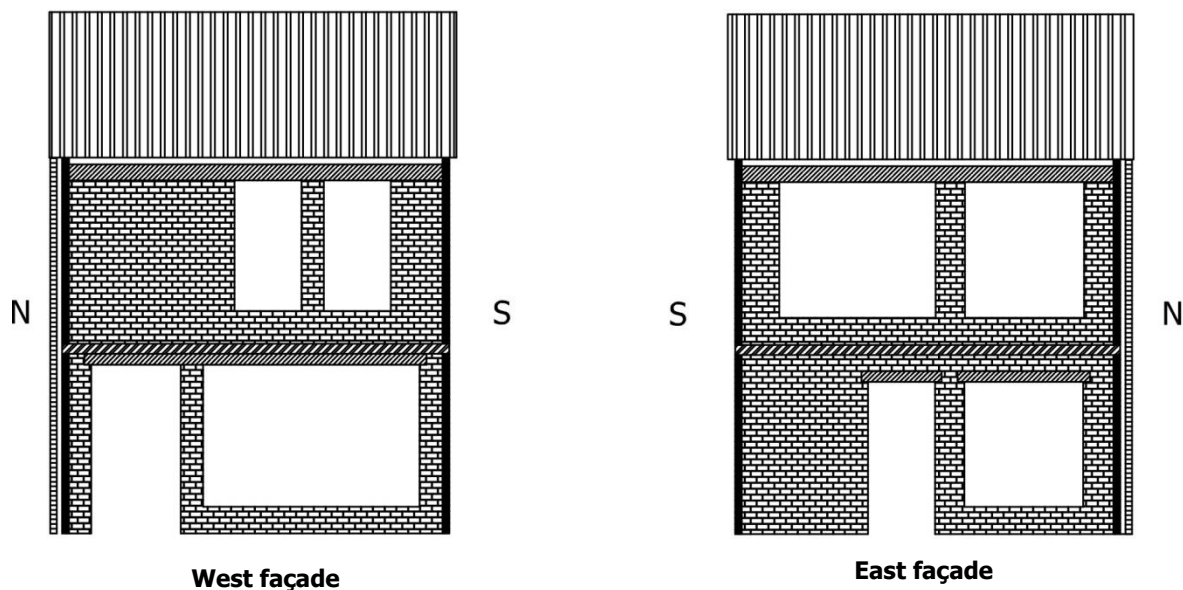


Figure 2. Layout of the front (west) and back (east) façades of the EUC-BUILD-6 building (for sake of convenience, vertical sections looking at the CS inner leaf are shown)

3 Set of variations used for the validation study

The current project aims to compare the results of NLFEA NLPO analyses performed with DIANA FEA 10.3, with those computed following the SLAMA method for a generic terraced house. For this reason, a number of variations are introduced consistently to the reference building, and the comparison is performed for each of these variations. In addition, a single façade is studied in order to determine where the difference with the results obtained by the more sophisticated analyses come from: whether from the assessment of a 2D perforated wall or from other points, such as the connection with the transversal walls (i.e. the flange effect) or the redistribution of forces between the façades.

3.1 Complete building

When a 3D analysis of the complete building is performed, the most relevant variation for the considered typology regards the number of storeys of the building. The reference building described in Section 2 is a two-storey building. Alternatively, *a one-storey building* constituted of the reference building without the second storey is analysed. The other variations proposed in this plan of approach are listed below. For every variation, both a uniform and a modal pattern of the lateral load distribution are considered, for both the positive and negative direction. A total of 48 variations is then obtained, as summarised in Table 3.

- i. **Building regularity (layout of the façades).** Four different combinations of the front and back façades are considered, including the reference building. The variations are defined as a combination of the East Façade (EF) and West Façade (WF) of the reference building. The considered combinations are reported in Table 1 and shown visually in Table 2.
- ii. **Masonry type (material properties).** Two URM types are considered: Calcium Silicate (CS) bricks with general purpose mortar and CS elements with thin layer mortar. The material properties are defined according to Table F.2 of NPR 9998.
- iii. **Floor type.** Two floors combinations are considered:
 - a. A reinforce concrete (RC) floor at first level and a timber (T) floor at the attic level (reference building): RC-T.
 - b. A RC floors at both first level and attic level: RC-RC.
 This variation does not apply to the single storey building, for which only a RC attic is considered.
- iv. **Structural continuity of the façades.** In the reference building, the RC slab at first level interrupts the walls of the two façades (even though in static conditions the gravity loads are transferred only to the transversal walls). Alternatively, a unidirectional RC slab that spans between the transversal walls and is connected to the façades by means of anchors to prevent the out-of-plane behaviour only (similar to the solution adopted in the test performed at TU Delft [9], as shown in Figure 3) is considered.

Table 1. Different combinations of façades.

Combination	West façade	East façade	Regularity	
			Plan	Elevation
C1	WF	EF	No	No
C2	WF	WF	Yes	No
C2*	WF*	WF*	Yes	No
C3	EF	EF	Yes	No

WF, EF = west and east façade of the reference building

WF* = west façade of the reference building without the central pier

Table 2. Visual representation of the different combinations of façades analysed.

Combination	Front (west) façade	Back (east) façade	% openings
C1			Ground storey: 65% First storey: 53%
C2			Ground storey: 81% First storey: 35%
C2*			Ground storey: 87% First storey: 35%
C3			Ground storey: 48% First storey: 71%

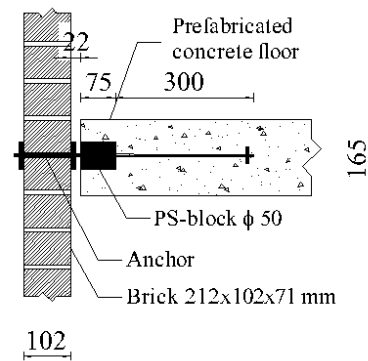


Figure 3. Detail of the floor-to-façade connection in the CS assemblage tested at TU Delft [9].

Table 3. Complete list of the 24 variations performed for the complete building for the positive loading direction. For the negative loading direction, the same variations are considered.

No.	Name	No. Storeys	Regularity	Masonry type	Floor type	Continuity of façades	Load distribution
#1	2S/WE/CSB/RC-T/D/UP	2 storeys	WF-EF	CS bricks	RC-T	Discontinuous	Uniform pattern
#2	2S/WW/CSB/RC-T/D/UP	2 storeys	WF-WF	CS bricks	RC-T	Discontinuous	Uniform pattern
#3	2S/WW*/CSB/RC-T/D/UP	2 storeys	WF*-WF*	CS bricks	RC-T	Discontinuous	Uniform pattern
#4	2S/EE/CSB/RC-T/D/UP	2 storeys	EF-EF	CS bricks	RC-T	Discontinuous	Uniform pattern
#5	2S/WE/CSE/RC-T/D/UP	2 storeys	WF-EF	CS elements	RC-T	Discontinuous	Uniform pattern
#6	2S/WE/CSB/RC-RC/D/UP	2 storeys	WF-EF	CS bricks	RC-RC	Discontinuous	Uniform pattern
#7	2S/WE/CSB/RC-T/C/UP	2 storeys	WF-EF	CS bricks	RC-T	Continuous	Uniform pattern
#8	2S/WE/CSB/RC-T/D/MP	2 storeys	WF-EF	CS bricks	RC-T	Discontinuous	Modal pattern
#9	2S/WW/CSB/RC-T/D/ MP	2 storeys	WF-WF	CS bricks	RC-T	Discontinuous	Modal pattern
#10	2S/WW*/CSB/RC-T/D/ MP	2 storeys	WF*-WF*	CS bricks	RC-T	Discontinuous	Modal pattern
#11	2S/EE/CSB/RC-T/D/ MP	2 storeys	EF-EF	CS bricks	RC-T	Discontinuous	Modal pattern
#12	2S/WE/CSE/RC-T/D/ MP	2 storeys	WF-EF	CS elements	RC-T	Discontinuous	Modal pattern
#13	2S/WE/CSB/RC-RC/D/ MP	2 storeys	WF-EF	CS bricks	RC-RC	Discontinuous	Modal pattern
#14	2S/WE/CSB/RC-T/C/ MP	2 storeys	WF-EF	CS bricks	RC-T	Continuous	Modal pattern
#15	1S/WE/CSB/RC/UP	1 storey	WF-EF	CS bricks	RC	-	Uniform pattern
#16	1S/WW/CSB/RC/UP	1 storey	WF-WF	CS bricks	RC	-	Uniform pattern
#17	1S/WW*/CSB/RC/UP	1 storey	WF*-WF*	CS bricks	RC	-	Uniform pattern
#18	1S/EE/CSB/RC/UP	1 storey	EF-EF	CS bricks	RC	-	Uniform pattern
#19	1S/WE/CSE/RC/UP	1 storey	WF-EF	CS elements	RC	-	Uniform pattern
#20	1S/WE/CSB/RC/MP	1 storey	WF-EF	CS bricks	RC	-	Modal pattern
#21	1S/WW/CSB/RC/ MP	1 storey	WF-WF	CS bricks	RC	-	Modal pattern
#22	1S/WW*/CSB/RC/MP	1 storey	WF*-WF*	CS bricks	RC	-	Modal pattern
#23	1S/EE/CSB/RC/MP	1 storey	EF-EF	CS bricks	RC	-	Modal pattern
#24	1S/WE/CSE/RC/MP	1 storey	WF-EF	CS elements	RC	-	Modal pattern

WF* = West façade without the central pier at ground floor, as shown for variation C2* in Table 2.

For the one-storey building, WF and EF must be intended as the ground floor part of the façades of the reference building.

3.2 Single façade

For the 2D analyses of a façade, the west façade of the reference building is considered. Given the lower computational effort, for the 2D analyses all the variations are combined systematically and a much larger

total number of combinations is then obtained (1040 façades are analysed). The analysis of each variation is carried out for both the positive and negative loading direction.

1. **Geometry of the façade.** The influence of the dimensions of the central pier at ground floor on the overall wall capacity is studied. A combination of two sets of variations are considered:
 - Length of the pier: the length is increased in 3 steps from a minimum value of 0.33 m (ref wall) to a maximum value of 2.13 m, with an intermediate step of 0.8 m. The pier lengths are selected to align the pier with the openings of the upper level.
 - Height of the window bank: the height is increased in 3 regular steps from a minimum value of 0.4 m (ref wall) to a maximum value of 0.8 m, with an intermediate value of 0.6 m.

A façade without the central pier (and hence the window bank) is considered in addition.

In total, 13 cases are considered, each one characterized by a different aspect ratio of the central pier of the ground storey. When the single-storey façade is analysed, the ground floor portion of each of the 13 variations is considered.

2. **Masonry type.** The material properties used for the 3D analyses are considered (see Section 3.1).
3. **Floor type.** The same variations considered for the 3D analyses are considered (see Section 3.1).
4. **Structural continuity of the façade.** Similar to the 3D analyses (see Section 3.1).
5. **Distribution of lateral loads.** Four different types of lateral load distributions are considered. In addition to the standard uniform and modal patterns distributed proportionally to the mass along the height of the façade, also two distributions with the lateral loads applied only at the floor levels are modelled and computed according to either a uniform or a modal pattern.

More details and the graphical representation of the variations listed above can be found in the plan of approach [8].

4 Methodology used for SLaMA and NLFEA

4.1 SLaMA models

The SLaMA analyses are performed according to the procedure and the equations recommended in Annex G of NPR 9998:2018 [1]. Each analysis follows the following steps:

- Each perforated wall (i.e. each façade) is divided into single elements. The meshing procedure follows the recommendations reported in Section G.9.2.1, based on the identification of the compressive struts in the walls (Figure 4a). An example of the mesh of the west façade is presented in Figure 4b, where the piers of the top storey are conservatively assumed to be cantilever due to the lack of spandrels and the presence of a flexible timber floor at the attic level. The piers at the ground storey are assumed to be double hinged due to the presence of the stiff and strong RC floor and of the concrete lintels.
- The vertical loads acting on each piers and contributing to the structural stability are computed.
- The force-displacement behaviour of each pier is computed. The second order effects are taken into account as reported in Section 4.4.2.2 of NPR 9998:2018 [1].
- The capacity of each single façade is evaluated separately for every storey. That is computed by summing up the capacity of the individual members at that level. An example is shown in Figure 5.
- The capacity of the structure is then computed for the whole building at each storey level. When the floor is sufficiently stiff to provide a box-behaviour, the contribution of the two facades is considered by taking into account the eccentricity of each of them with respect the centre of stiffness of that level.
- The capacity is scaled by the effective mass of the sub-structure (in this case, either the whole building or the top storey only), computed as recommended in [10] and shown in Figure 6. The capacity of the two sub-systems is then presented in terms of accelerations and a comparison is made to identify the sub-structure whose failure is governing (i.e. has the lowest capacity) (Figure 7a).
- The governing capacity curve is scaled up by the effective mass of the total structure, and the equivalent bilinear curve is computed in accordance with the recommendations of Section G.4.2 of NPR 9998:2018 [1].

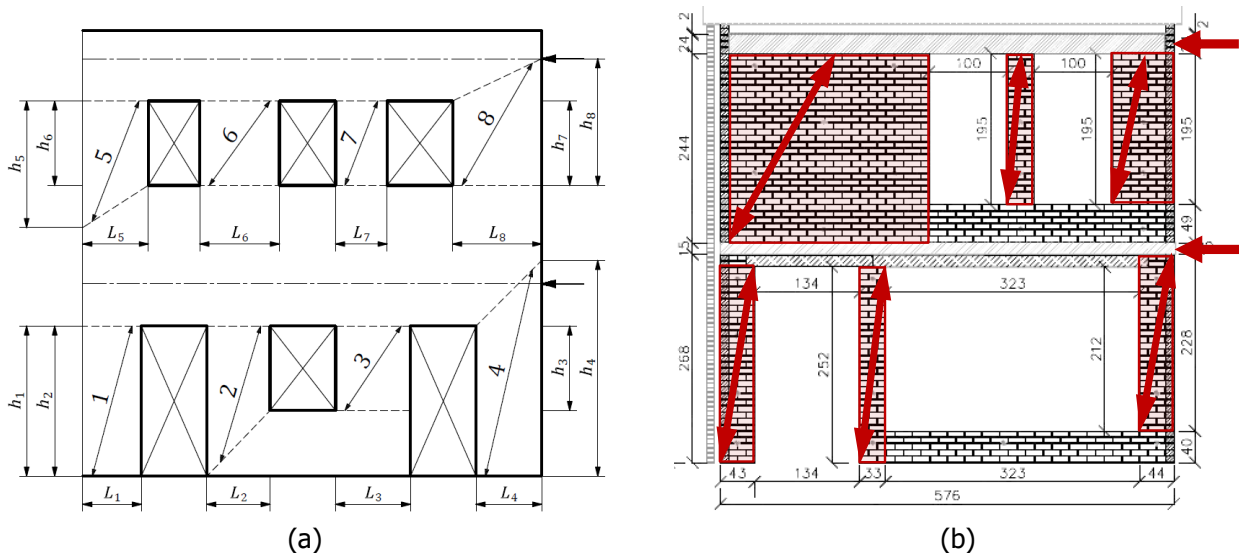


Figure 4. Graphical representation of the compressive struts of a perforated wall as recommended in [1] (a), and example of meshing on the West façade of the reference building (b).

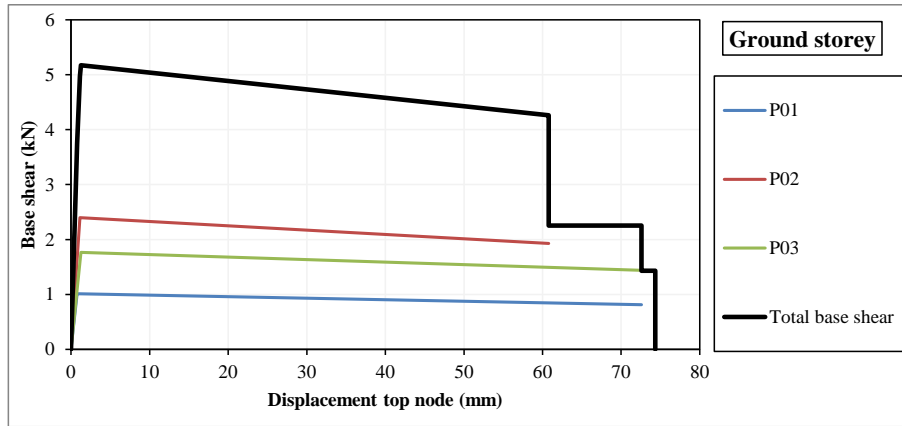


Figure 5. Example of capacity of the ground storey level of a perforated wall (West façade).

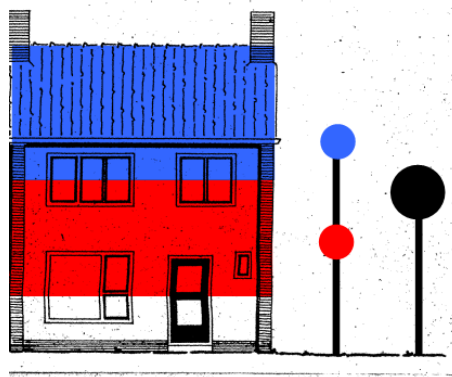


Figure 6. Seismic mass lumped at different storey levels (from [10]).

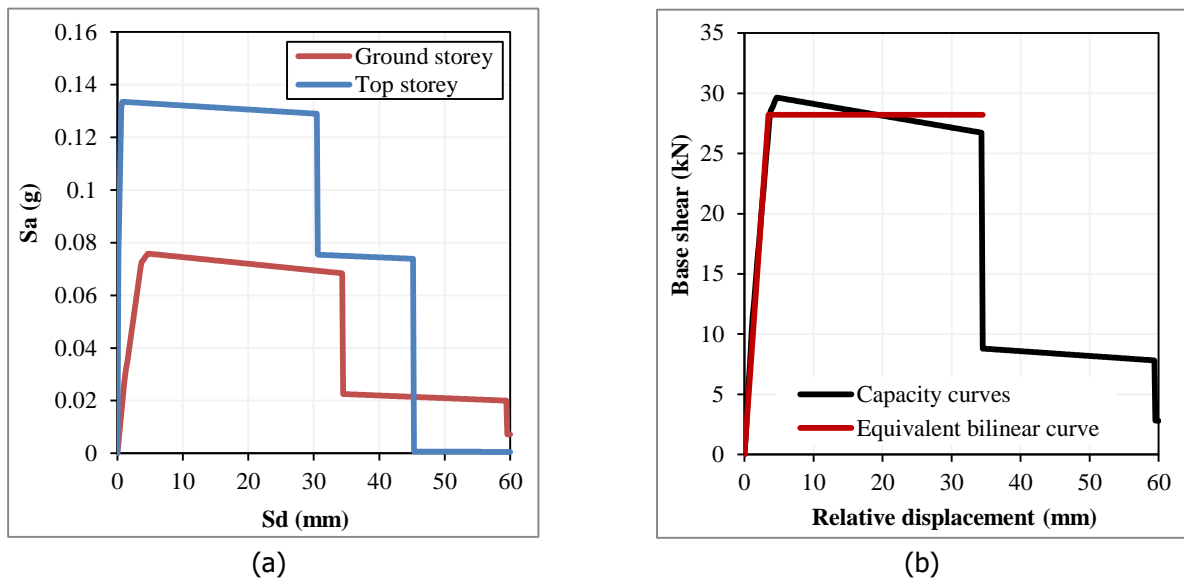


Figure 7. Capacity curve for each storey level (a): the ground storey capacity is governing. Final capacity curve in terms of base shear forces and equivalent bilinear curve (b).

4.2 Finite Element models in Diana 10.3

The terraced house representing the EUC-BUILD-6 is numerically modelled in 2D and 3D by the software Diana 10.3. Quadratic 8-noded curved shell elements (CQ40S and CT30S) are used to model walls, floors and lintels of the 3D building. The timber beams in the roof or in the attic floor are modelled with linear Class-III beam element (CL18B). A non-linear constitutive behaviour is considered for the masonry walls, while the rest of the elements are linear elastic. Two different material models are used for the masonry: the Engineering Masonry Model for the CS brick masonry, and the Total Strain Rotating Crack Model (including Coulomb-Friction interface elements at wall connection corners) for the CS element masonry. The material properties of masonry are taken from Table F.2 of NPR 9998:2018 [1]. An orthotropic behaviour, whose properties are calibrated according to the laboratory experiment, is assigned to timber planks of the floor and the roof. Mass densities are selected in order to match the experimental specimen mass. The mass of the outer North leaf is included in the North façade. The model is restrained at the bottom from translations and rotations. The elements are meshed with an average size of 200x200 mm (an example of the mesh, for case study #01, is depicted in Figure 8). Unlike the 3D models, the approach for the 2D models makes use of quadratic 8-noded plane stress elements (CQ16M and CT12M) to model the West façade. The elements corresponding to the floors are modelled with a fictitious thickness (1 m) such that the higher stiffness compared to the walls is taken into account. The mass density of these elements is adapted to consider the actual gravity loads acting on the walls. The mesh size is reduced to 100x100 mm. Two examples of meshes 2D models are depicted in Figure 9.

Non-linear static analyses are performed for both 2D and 3D models. The model is initially subjected to the gravity loads in ten equal steps. Then, either uniform distributed lateral loads, applied via a uniform lateral acceleration, or modal distributed lateral loads, based on the main eigen-mode (and the corresponding participating mass) of the structure obtained via eigen-value analyses, is applied such that an average displacement rate of 0.1 mm/step is recorded at floor level. The Secant BFGS (Quasi-Newton) method is adopted as iterative method in combination with the Arc-Length control. Both displacement and force norms must be satisfied during the iterative procedure within a tolerance of 1%. The Parallel Direct Sparse method is employed to solve the system of equations. The second order effects are considered via the Total Lagrange geometrical nonlinearity.

The force-displacement curve of the building is extrapolated for each storey level and the equivalent bilinear curve is computed according to the procedure recommended in Section G.4.2 of NPR 9998:2018 [7] and summarised for the SLAMA method. Examples of capacity curves for both 2D and 3D analyses are shown in Figure 10.

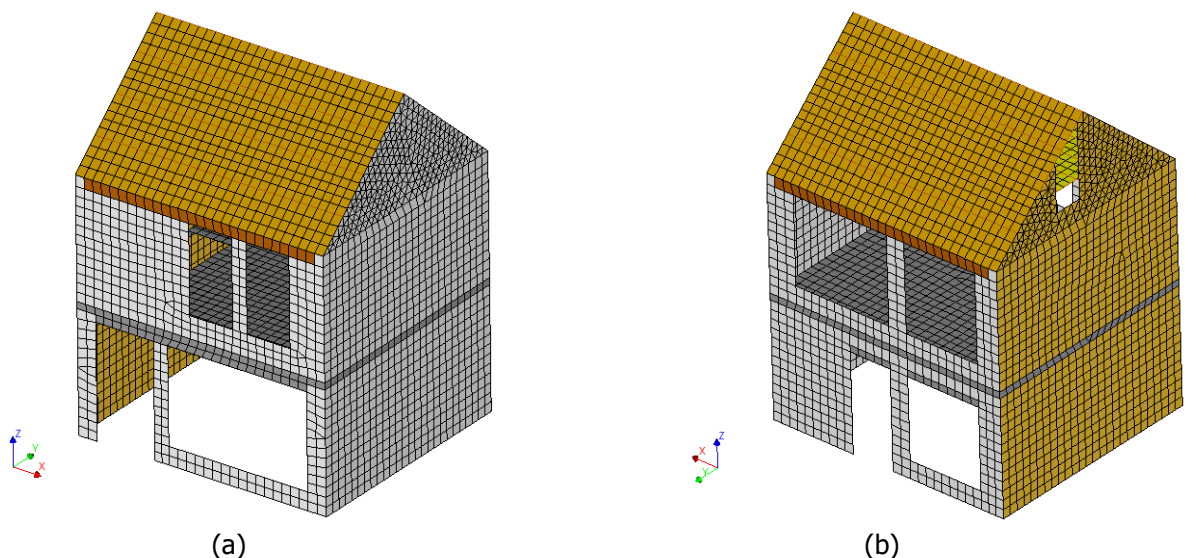


Figure 8. Diana 3D model of case study #01. South-West view (a) and North-East view (b).

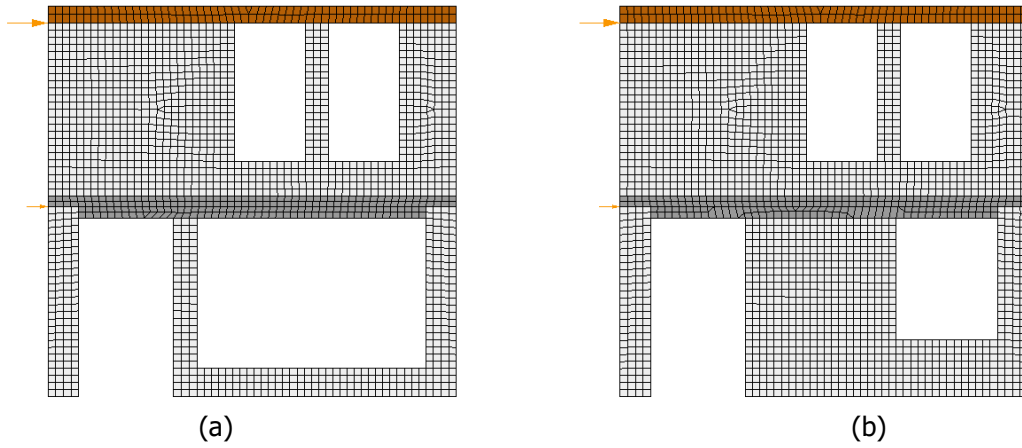


Figure 9. Diana 2D models. Case study #01 with original pier length of 0.33m and bank height of 0.4m (a) and pier length of 2.33m and bank height of 0.8m (b).

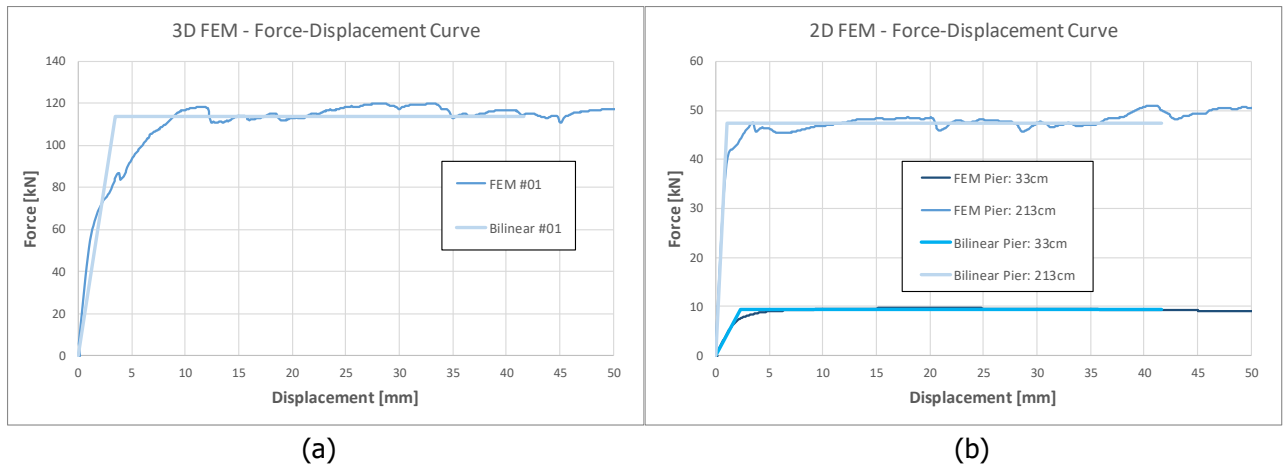


Figure 10. Force-displacement curves of 3D NLFEA (a) and 2D NLFEA (b).

5 Comparison of the results

5.1 3D analyses

The results of the 48 analyses performed for the whole building are summarised in Table 4 and Table 5, and shown in Figure 11 in terms of equivalent bilinear curve. Refer to Section 3.1 for the description of the characteristics of the building analysed in each analysis. The average and standard deviation values reported at the bottom of the table are computed assuming a lognormal distribution, that can better approximate the results than a normal distribution. Similarly, the average curves plotted in Figure 11 refer to the lognormal distribution. Figure 12 shows a comparison between the equivalent lognormal distributions defined for (i) the initial stiffness, (ii) the near collapse displacement, and (iii) the ultimate base shear, computed based on the results of the analyses performed with NLFEA and SLaMA.

For the large majority of the analyses, the same failure mode, generally governed by flexure, is obtained for both the methods. The crack pattern of the reference case study (#01) for the NLFEA is shown in Figure 13, and compared to the failure mode predicted by the SLaMA method.

Table 4. Results of SLaMA and NLFEA for positive pushover curves.

Case #	K_{in} (kN/mm)		d_y (mm)		d_{nc} (mm)		V_u (kN)	
	SLaMA	NLFEA	SLaMA	NLFEA	SLaMA	NLFEA	SLaMA	NLFEA
1	26.3	33.0	1.45	3.45	49.4	41.6	38.0	113.8
2	7.5	13.9	2.77	4.73	54.3	41.6	20.8	65.7
3	5.7	9.9	3.20	5.91	46.5	41.6	18.4	58.4
4	34.7	30.2	0.77	3.80	48.9	41.6	26.7	114.5
5	26.3	49.6	1.47	3.04	54.3	41.6	38.8	150.5
6	31.6	26.6	1.66	5.11	32.7	41.6	52.3	135.9
7	15.9	15.8	1.42	6.38	50.9	41.6	22.6	101.0
8	26.4	21.1	1.45	5.07	49.4	41.6	38.2	107.0
9	7.5	12.3	2.77	4.86	54.3	41.6	20.9	59.5
10	5.8	8.9	3.20	6.07	46.5	41.6	18.4	53.8
11	27.2	14.4	0.77	3.59	48.9	41.6	20.9	51.7
12	26.3	39.1	1.47	3.25	54.3	33.8	38.8	127.2
13	31.6	22.3	1.66	5.60	32.7	41.6	52.3	124.7
14	15.9	12.5	1.42	7.13	50.9	41.6	22.6	89.0
15	24.2	67.2	1.23	1.42	52.1	41.6	29.8	95.5
16	6.5	15.4	2.42	3.31	58.8	41.6	15.6	50.8
17	5.5	10.3	2.67	4.49	52.1	41.6	14.8	46.5
18	40.6	164.4	1.07	0.79	33.5	25.5	43.5	130.5
19	68.8	74.7	0.64	1.61	33.9	41.6	43.7	120.4
20	24.2	54.9	1.23	1.53	52.1	41.6	29.8	83.9
21	6.5	13.2	2.42	3.31	58.8	41.6	15.6	43.9
22	5.5	9.0	2.67	4.55	52.1	41.6	14.8	41.1
23	40.6	158.3	1.07	0.69	33.5	16.7	43.5	109.2
24	68.8	63.5	0.64	1.78	33.9	14.4	43.7	112.9
Average¹	18.0	26.0	1.55	3.25	46.4	37.2	27.7	84.4

¹ the average is computed assuming a lognormal distribution

Table 5. Results of SLaMA and NLFEA for negative pushover curves (in absolute value).

Case #	K_{in} (kN/mm)		d_y (mm)		d_{NC} (mm)		V_u (kN)	
	SLaMA	NLFEA	SLaMA	NLFEA	SLaMA	NLFEA	SLaMA	NLFEA
1	69.4	45.0	0.59	2.32	45.3	41.6	40.8	104.6
2	8.1	13.3	3.47	4.83	34.5	41.6	28.2	64.5
3	8.2	10.9	3.25	5.29	30.5	41.6	26.8	57.4
4	22.8	35.4	0.97	2.99	51.9	41.6	22.0	105.8
5	69.5	97.9	0.59	1.14	47.3	28.5	41.3	111.4
6	64.8	46.7	1.25	2.56	31.8	41.6	81.1	119.8
7	70.1	31.0	0.59	3.00	45.3	30.0	41.3	93.1
8	54.4	33.2	0.59	2.63	45.3	29.5	32.0	87.4
9	23.3	12.0	1.66	4.85	34.5	41.6	38.7	58.1
10	8.0	9.8	3.25	5.38	30.5	41.6	26.1	52.5
11	17.9	18.0	0.97	2.55	51.9	41.6	17.2	45.9
12	54.5	75.0	0.59	1.24	47.3	24.1	32.4	92.8
13	132.4	39.3	0.57	2.77	29.7	41.6	76.1	109.0
14	54.7	24.9	0.59	3.09	45.3	25.3	32.2	76.8
15	63.7	75.0	0.68	1.16	34.4	41.6	43.6	87.0
16	7.5	15.5	2.24	3.05	50.6	41.6	16.7	47.3
17	8.3	10.7	2.17	4.00	46.7	41.6	18.0	42.7
18	128.3	175.9	0.55	0.73	34.2	41.6	70.4	127.6
19	63.7	152.5	0.69	0.62	35.4	27.1	43.9	94.8
20	63.7	61.6	0.68	1.24	34.4	41.6	43.6	76.6
21	7.5	12.9	2.24	3.15	50.6	41.6	16.7	40.8
22	8.3	9.4	2.17	4.02	46.7	41.6	18.0	37.7
23	128.3	159.0	0.55	0.71	34.2	16.7	70.4	113.4
24	63.7	129.5	0.69	0.63	35.4	23.1	43.9	81.5
Average¹	32.8	34.6	1.04	2.18	39.8	35.2	34.2	75.3

¹ the average is computed assuming a lognormal distribution

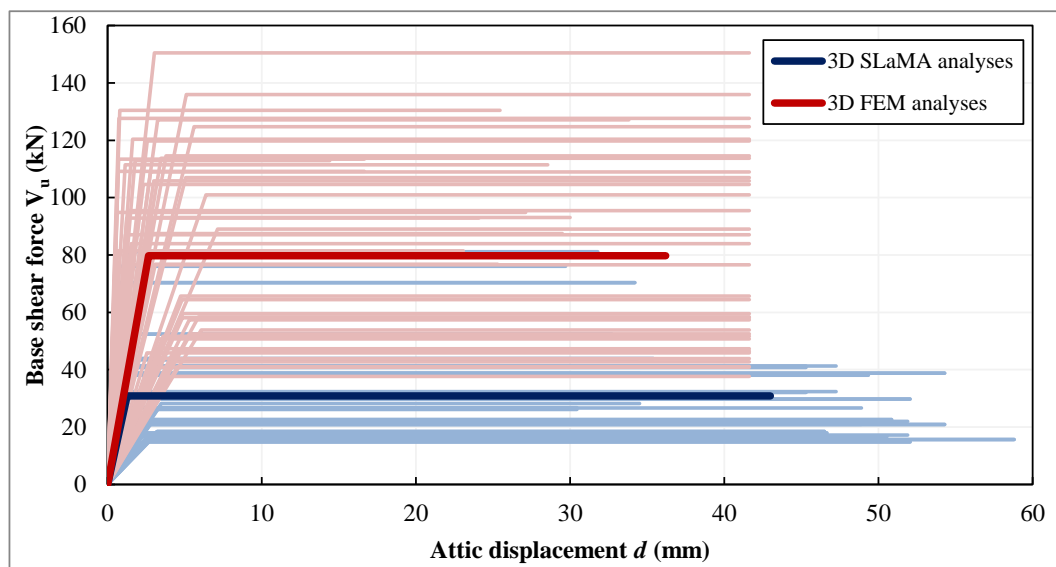


Figure 11. Bilinear curves computed for NLFEA and SLaMA analyses (average curves are thicker and darker).

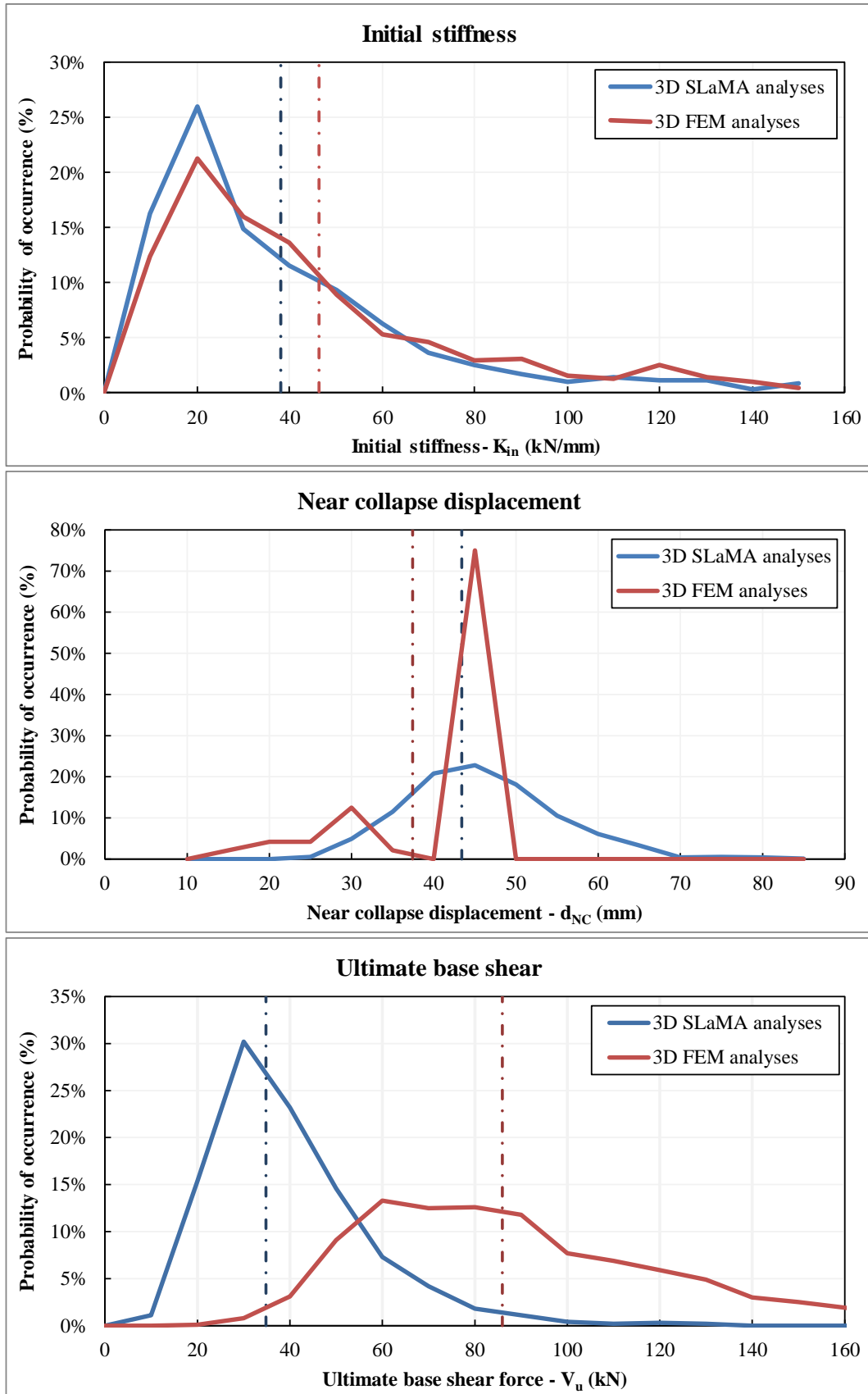


Figure 12. Comparison between the equivalent lognormal distributions of (i) initial stiffness, (ii) near collapse displacement (for the NLFEA the original data were considered), and (iii) ultimate base shear computed for all the 48 analyses with 3D NLFEA and SLaMA. The dash-dot lines indicate the average values. The probability of occurrence is considered for discrete intervals of 10 kN/mm, 5 mm, 10 kN, respectively.

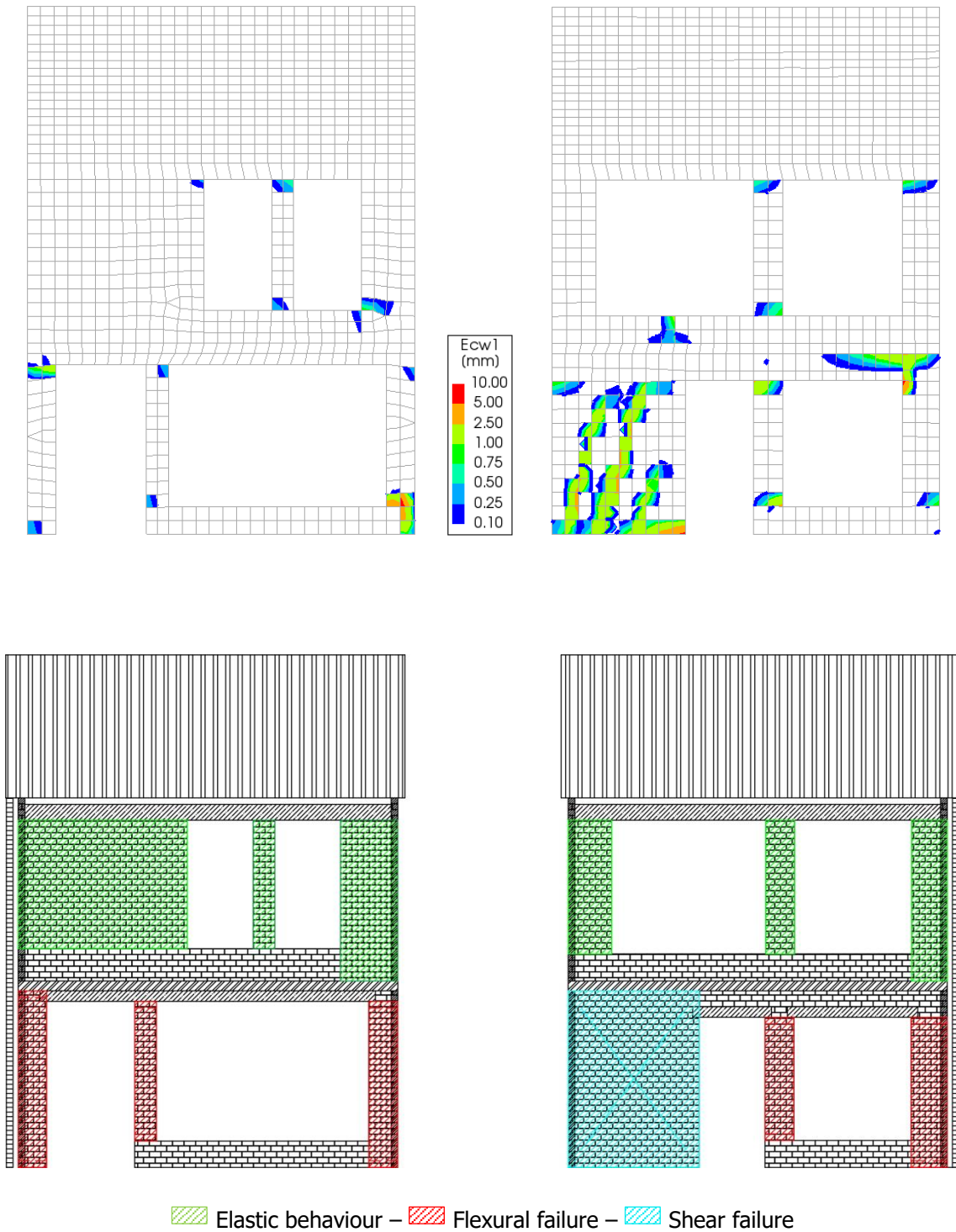


Figure 13. Crack pattern at peak load for case study #01 obtained from the NLFEA and compared to the failure mode predicted by the SLaMA method.

The results show that, despite significant differences are observed when the single cases are compared, an acceptable agreement between the analyses is obtained on average in terms of the initial stiffness and of the

displacement capacity. In the NLFEA, the near collapse displacement capacity was very often limited by the global drift limit at inter-storey level (1.5% for ductile mechanisms), and for this reason the capacity of most of the analysed buildings was slightly larger than 40 mm. This value is very close to the average near collapse displacement computed for the SLaMA analyses, which was limited by the flexural displacement capacity of the single piers. The results presented confirms then that the use of the global drift limit for ductile mechanisms reported in Table G.2 of NPR 9998 [1] (that must be applied with NLFEA) provides results on average similar to those obtained at the single wall level according to Eq. (G.31) (that is used with the SLaMA method).

On the other hand, large differences are observed when the ultimate base shear is compared. The NLFEA return a base shear capacity on average more than 2.5 times higher than those computed according to the SLaMA method.

These observations are overall confirmed when the results are compared individually one by one, as reported in Table 6, and by the plot of the cumulative distribution functions for the ratio computed for the results of NLFEA and SLaMA analyses (Figure 14), where it is observed as the ratio between the ultimate base shear computed according to a NLFEA and a SLaMA analysis is larger than 1.5 for more than 95% of the analyses performed.

More detailed comments, with the analysis of the influence of the different variations on the obtained results, are provided in Section 5.2 after the presentation of the results obtained for the 2D analyses.

Table 6. Ratio between the results obtained with the SLaMA and NLFEA (red background for larger values, green background for small values).

Case #	NLFEA/SLaMA							
	K_{in} (kN/mm)		d_y (mm)		d_{NC} (mm)		V_u (kN)	
	Positive	Negative	Positive	Negative	Positive	Negative	Positive	Negative
1	1.25	0.65	2.38	3.93	0.84	0.92	2.99	2.56
2	1.85	1.64	1.71	1.39	0.77	1.21	3.16	2.29
3	1.74	1.33	1.85	1.63	0.89	1.36	3.17	2.14
4	0.87	1.55	4.94	3.08	0.85	0.80	4.29	4.81
5	1.89	1.41	2.07	1.93	0.77	0.60	3.88	2.70
6	0.84	0.72	3.08	2.05	1.27	1.31	2.60	1.48
7	0.99	0.44	4.49	5.08	0.82	0.66	4.47	2.25
8	0.80	0.61	3.50	4.46	0.84	0.65	2.80	2.73
9	1.64	0.52	1.75	2.92	0.77	1.21	2.85	1.50
10	1.53	1.23	1.90	1.66	0.89	1.36	2.92	2.01
11	0.53	1.01	4.66	2.63	0.85	0.80	2.47	2.67
12	1.49	1.38	2.21	2.10	0.62	0.51	3.28	2.86
13	0.71	0.30	3.37	4.86	1.27	1.40	2.38	1.43
14	0.79	0.46	5.02	5.24	0.82	0.56	3.94	2.39
15	2.78	1.18	1.15	1.71	0.80	1.21	3.20	2.00
16	2.37	2.07	1.37	1.36	0.71	0.82	3.26	2.83
17	1.87	1.29	1.68	1.84	0.80	0.89	3.14	2.37
18	4.05	1.37	0.74	1.33	0.76	1.22	3.00	1.81
19	1.09	2.39	2.52	0.90	1.23	0.77	2.76	2.16
20	2.27	0.97	1.24	1.82	0.80	1.21	2.82	1.76
21	2.03	1.72	1.37	1.41	0.71	0.82	2.81	2.44
22	1.64	1.13	1.70	1.85	0.80	0.89	2.78	2.09
23	3.90	1.24	0.64	1.29	0.50	0.49	2.51	1.61
24	0.92	2.03	2.78	0.91	0.42	0.65	2.58	1.86
Average	1.44	1.05	2.10	2.10	0.80	0.88	3.05	2.20

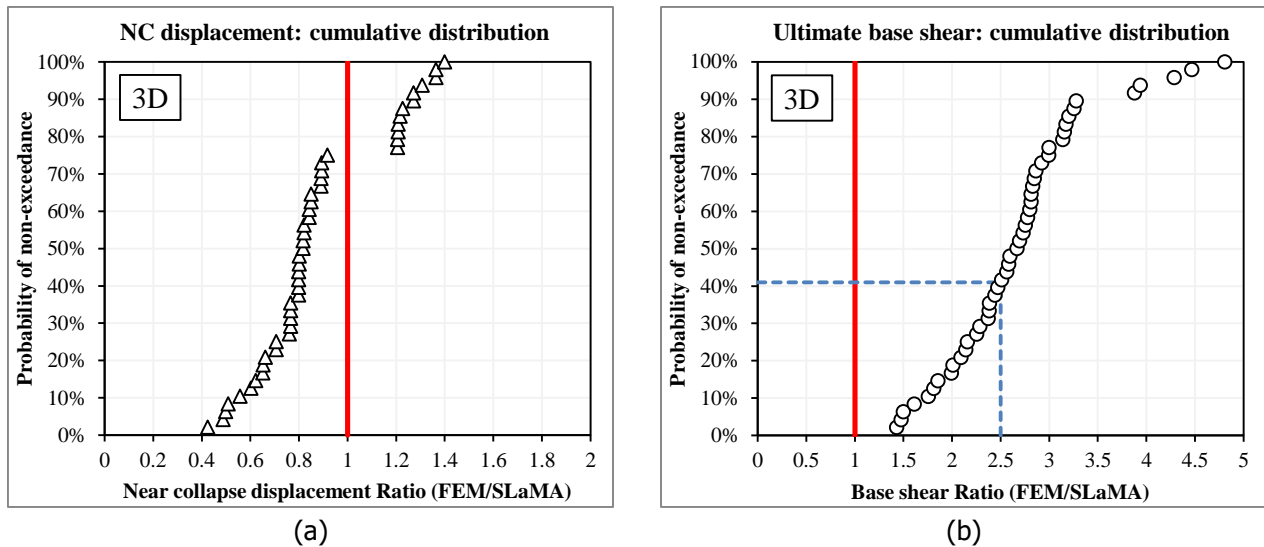


Figure 14. Cumulative distribution functions for the ratio computed for the results of 3D NLFEA and SLaMA analyses: near collapse displacement (a) and ultimate base shear (b). For instance, a probability of non-exceedance of 0.41 is obtained for a base shear ratio between the results of NLFEA and SLaMA equal to 2.5 (i.e. the ratio is larger than 2.5 in almost 60% of the cases).

5.2 2D analyses

Given the large number of analyses performed, the results for the 2D analyses are presented in terms of aggregate data. Besides, these analyses are mainly used to evaluate the influence of the variations presented in Section 3 on the capacity of the buildings computed according to the NLFEA and SLaMA analyses. Specific attention is devoted to the ultimate base shear, because it is the parameters that presents the largest discrepancies between the NLFEA and SLaMA analyses for the 3D analyses of the complete building.

Figure 15 shows a comparison between the equivalent lognormal distributions of (i) initial stiffness, (ii) near collapse displacement (for the NLFEA the original data were considered), and (iii) ultimate base shear computed for all the analyses with NLFEA and SLaMA. Overall the results are in line with those observed for the 3D analyses:

- similar values of the initial stiffness are obtained for both the computational methods;
- the near collapse displacements of the NLFEA are again often limited by the global drift limits recommended in Table G.2 of NPR 9998. Similar to the 3D analyses, the value recommended for ductile mechanisms is close to the average value obtained for the SLaMA analyses (also shown in Figure 16);
- the difference between the values of the ultimate base shear computed according to the two methods is smaller (around 1.5, as shown in Figure 16), although a large dispersion of the results is observed: in fact, for some specific analyses a factor larger than 8 is computed (Table 7 and Table 8).

The differences between the results of the 2D and 3D analyses mainly depend on the smaller gravity loads acting on the piers and by the absence of the connection at corners with the transversal walls when the single façades are investigated. This point enhances how relevant is the load redistribution between different walls, wither in the same direction (i.e. between the two façades) or between walls that are orthogonal with each other. In fact, although the method proposed by Moon et al [11] is used to account for the influence of the flanges on the rocking capacity of the piers, the SLaMA method seems not to be able to fully capture this effect.

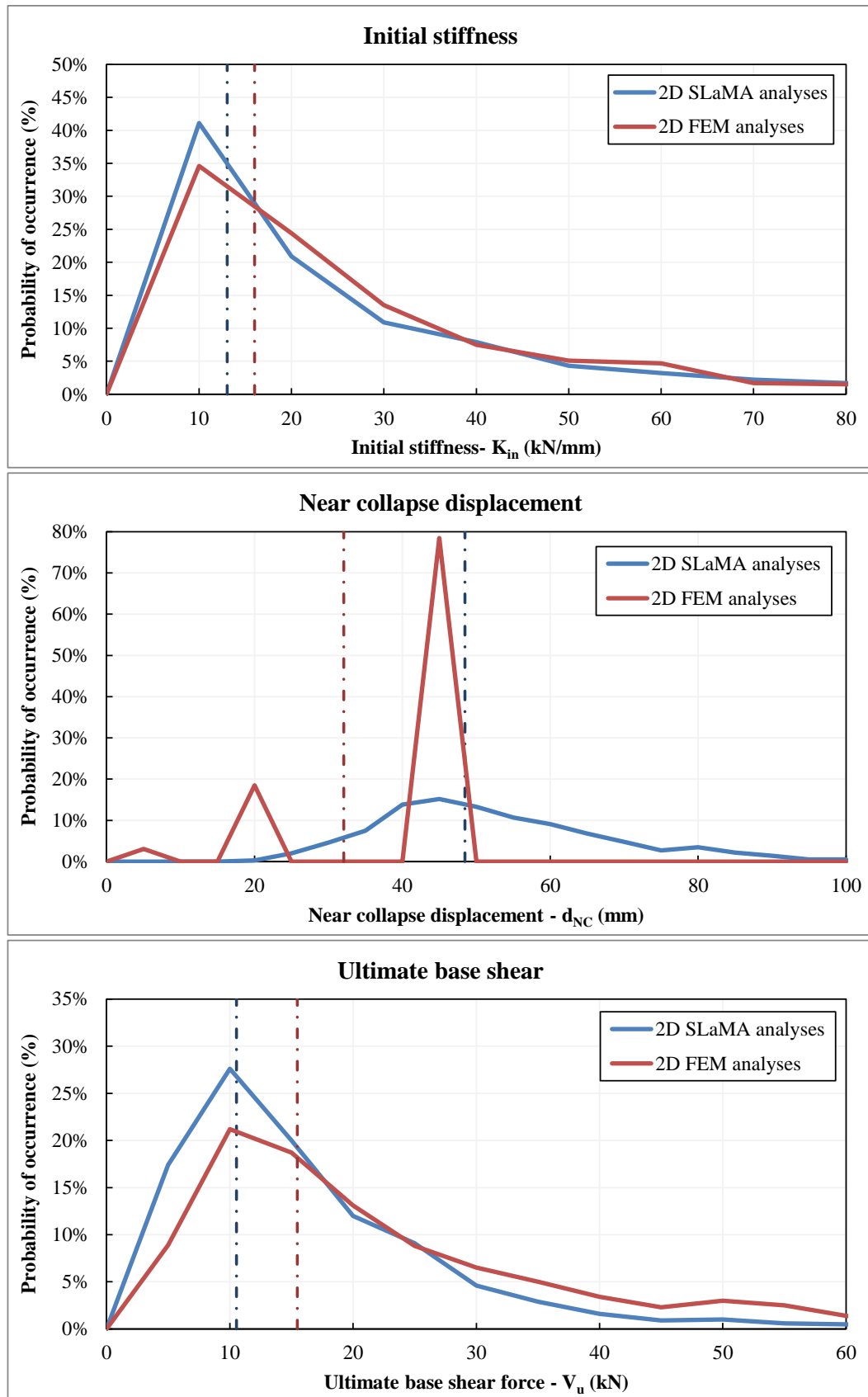


Figure 15. Comparison between the equivalent lognormal distributions of (i) initial stiffness, (ii) near collapse displacement (for the NLFEA the original data were considered), and (iii) ultimate base shear computed for all the 1040 analyses with 2D NLFEA and SLaMA. The dash-dot lines indicate the average values. The probability of occurrence is considered for discrete intervals of 10 kN/mm, 5 mm, 10 kN, respectively.

Table 7. Ratio between the ultimate base shear computed with the NLFEA and the SLaMA analyses, respectively, for the positive loading direction (red/green background for large/small values, respectively).

FEM/SLaMA ultimate base shear	WBH1						WBH2						WBH3						WBH4						
	1 storey			2 storeys			1 storey			2 storeys			1 storey			2 storeys			1 storey			2 storeys			
	RC	T	C-T	RC-RC	RC-T	C-T	RC	T	C-T	RC-RC	RC-T	C-T	RC	T	C-T	RC-RC	RC-T	C-T	RC	T	C-T	RC-RC	RC-T	C-T	
CSB	MD	1.15	1.36	1.04	1.06	1.09	1.24	2.00	1.16	1.20	1.18	1.29	2.13	1.17	1.23	1.21	1.36	2.28	1.36	2.28	1.18	1.34	1.26	1.26	1.26
	UD	1.20	1.56	1.06	1.08	1.04	1.40	2.84	1.22	1.29	1.37	1.51	3.33	1.25	1.36	1.47	1.64	3.86	1.64	3.86	1.29	1.51	1.59	1.59	1.59
	UP	1.13	1.30	1.03	1.05	1.03	1.11	1.22	1.15	1.18	1.15	1.27	1.88	1.16	1.22	1.18	1.33	2.08	1.33	2.08	1.18	1.32	1.23	1.23	1.23
PL1	TC	1.13	1.30	1.03	1.05	1.03	1.11	1.22	1.15	1.18	1.15	1.27	1.88	1.16	1.22	1.18	1.33	2.08	1.33	2.08	1.18	1.32	1.24	1.24	1.24
	MD	1.22	2.39	1.08	1.12	1.22	1.22	1.76	1.15	1.18	1.15	1.27	1.88	1.16	1.22	1.18	1.33	2.08	1.33	2.08	1.18	1.32	1.24	1.24	1.24
	UD	1.29	2.67	1.09	1.15	1.28	1.22	4.13	1.15	1.20	1.58	1.32	4.39	1.17	1.22	1.64	1.40	4.61	1.40	4.61	1.21	1.36	1.73	1.73	1.73
CSE	UC	1.23	2.37	1.07	1.12	1.20	1.22	4.13	1.15	1.20	1.58	1.32	4.39	1.17	1.22	1.64	1.40	4.61	1.40	4.61	1.21	1.36	1.73	1.73	1.73
	TC	1.23	2.37	1.07	1.12	1.20	1.22	4.13	1.15	1.20	1.58	1.32	4.39	1.17	1.22	1.64	1.40	4.61	1.40	4.61	1.21	1.36	1.73	1.73	1.73
	MD	1.17	1.90	1.14	1.16	1.13	1.24	2.00	1.16	1.20	1.18	1.29	2.13	1.17	1.23	1.21	1.36	2.28	1.36	2.28	1.18	1.34	1.26	1.26	1.26
CSB	UD	1.24	2.21	1.17	1.20	1.21	1.40	2.84	1.22	1.29	1.37	1.51	3.33	1.25	1.36	1.47	1.64	3.86	1.64	3.86	1.29	1.51	1.59	1.59	1.59
	UC	1.17	1.75	1.14	1.15	1.11	1.22	1.76	1.15	1.18	1.15	1.27	1.88	1.16	1.22	1.18	1.33	2.08	1.33	2.08	1.18	1.32	1.23	1.23	1.23
	TC	1.17	1.75	1.14	1.14	1.11	1.22	1.76	1.15	1.18	1.15	1.27	1.88	1.16	1.22	1.18	1.33	2.08	1.33	2.08	1.18	1.32	1.24	1.24	1.24
PL2	MD	1.29	3.98	1.20	1.25	1.56	1.27	4.13	1.15	1.20	1.58	1.32	4.39	1.17	1.22	1.64	1.40	4.61	1.40	4.61	1.21	1.36	1.73	1.73	1.73
	UD	1.36	4.42	1.23	1.29	1.65	1.44	5.67	1.22	1.30	1.82	1.55	6.71	1.25	1.34	1.97	1.69	7.71	1.69	7.71	1.31	1.52	2.16	2.16	2.16
	UC	1.28	3.70	1.20	1.24	1.52	1.24	3.83	1.15	1.18	1.53	1.30	4.10	1.17	1.21	1.61	1.37	4.27	1.37	4.27	1.20	1.34	1.69	1.69	1.69
PL3	TC	1.28	3.70	1.19	1.24	1.52	1.24	3.83	1.15	1.18	1.53	1.30	4.10	1.17	1.21	1.61	1.37	4.27	1.37	4.27	1.20	1.34	1.69	1.69	1.69
	MD	1.30	2.18	1.12	1.20	1.22	1.44	2.48	1.18	1.28	1.32	1.50	2.59	1.20	1.32	1.37	1.56	2.73	1.56	2.73	1.22	1.44	1.41	1.41	1.41
	UD	1.39	2.57	1.17	1.26	1.34	1.63	3.47	1.26	1.39	1.57	1.76	3.93	1.30	1.47	1.68	1.89	4.27	1.89	4.27	1.34	1.63	1.80	1.80	1.80
PL4	UC	1.28	1.96	1.11	1.16	1.17	1.40	2.21	1.17	1.23	1.27	1.45	2.14	1.19	1.26	1.32	1.52	2.25	1.52	2.25	1.22	1.37	1.37	1.37	1.37
	TC	1.28	1.96	1.10	1.14	1.15	1.40	2.21	1.15	1.20	1.25	1.45	2.14	1.17	1.23	1.29	1.52	2.25	1.52	2.25	1.20	1.33	1.35	1.35	1.35
	MD	1.61	4.18	1.25	1.37	1.51	1.70	4.82	1.25	1.40	1.69	1.77	5.19	1.27	1.42	1.85	1.80	5.45	1.80	5.45	1.31	1.56	1.91	1.91	1.91
CSE	UD	1.73	4.85	1.29	1.44	1.71	1.95	6.91	1.34	1.52	2.01	2.07	7.75	1.37	1.59	2.24	2.28	8.74	2.28	8.74	1.44	1.76	2.46	2.46	2.46
	UC	1.57	4.07	1.24	1.32	1.51	1.73	4.50	1.24	1.32	1.75	1.77	4.80	1.28	1.37	1.83	1.80	5.07	1.80	5.07	1.30	1.48	1.90	1.90	1.90
	TC	1.57	4.07	1.22	1.30	1.53	1.73	4.50	1.22	1.31	1.73	1.77	4.80	1.24	1.33	1.80	1.80	5.07	1.80	5.07	1.25	1.43	1.87	1.87	1.87
CSB	MD	1.55	2.24	0.91	1.18	1.17	1.46	2.45	0.98	1.19	1.15	1.42	2.60	0.99	1.21	1.10	1.57	2.62	0.99	2.62	0.99	1.27	1.02	1.02	1.02
	UD	1.70	3.09	0.99	1.22	1.40	1.68	3.27	1.11	1.35	1.48	1.69	3.53	1.13	1.35	1.51	1.85	3.72	1.85	3.72	1.15	1.44	1.49	1.49	1.49
	UC	1.51	2.22	0.92	1.05	1.16	1.45	2.54	1.00	1.11	1.16	1.41	2.68	1.01	1.09	1.18	1.56	2.79	1.56	2.79	1.02	1.15	1.07	1.07	1.07
PL4	TC	1.51	2.22	0.88	0.96	1.04	1.45	2.54	0.95	1.05	1.07	1.41	2.68	0.96	1.03	1.08	1.56	2.79	1.56	2.79	0.96	1.09	0.97	0.97	0.97
	MD	2.26	4.70	1.15	1.60	1.68	2.60	5.64	1.21	1.74	1.81	2.72	6.12	1.18	1.78	1.79	2.69	6.29	2.69	6.29	1.16	1.79	1.74	1.74	1.74
	UD	2.74	5.90	1.33	1.76	2.05	2.91	7.09	1.41	1.92	2.30	3.08	8.04	1.41	1.98	2.40	3.31	8.58	3.31	8.58	1.44	2.15	2.46	2.46	2.46
CSE	UC	2.19	4.13	1.21	1.33	1.67	2.48	5.11	1.26	1.42	1.80	2.59	5.57	1.25	1.42	1.81	2.67	6.00	2.67	6.00	1.25	1.45	1.79	1.79	1.79
	TC	2.19	4.13	1.12	1.21	1.59	2.48	5.11	1.18	1.27	1.66	2.59	5.57	1.15	1.26	1.62	2.67	6.00	2.67	6.00	1.12	1.29	1.53	1.53	1.53

PL1, ..., PL4 = length of the central pier, as described in Section 3.2
 WBH1, ..., WBH4 = height of the window bank as described in Section 3.2
 CSB = Calcium Silicate Brick masonry; CSE = Calcium Silicate Element masonry
 RC = Reinforced concrete floor; T = timber floor; C = continuous façade
 MD = modal proportional distributed loads; UD = mass proportional distributed loads; UC = mass proportional concentrated loads; TC = triangular concentrated loads

Table 8. Ratio between the ultimate base shear computed with the NLFEA and the SLAMA analyses, respectively, for the negative loading direction (red/green background for large/small values, respectively).

FEM/SLAMA ultimate base shear	WBH1						WBH2						WBH3						WBH4									
	1 storey			2 storeys			1 storey			2 storeys			1 storey			2 storeys			1 storey			2 storeys						
	RC	T	RC-RC	RC-T	C-T	C-T	RC	T	RC-RC	RC-T	C-T	C-T	RC	T	RC-RC	RC-T	C-T	RC	T	RC-RC	RC-T	C-T	RC	T	RC-RC	RC-T	C-T	
Negative loading	MD	1.15	1.36	1.04	1.06	1.04																						
	UD	1.20	1.56	1.06	1.09	1.10																						
	UP	1.13	1.30	1.03	1.06	1.03																						
PL1	TC	1.13	1.30	1.03	1.05	1.03																						
	MD	1.22	2.39	1.08	1.13	1.24																						
	UD	1.29	2.67	1.10	1.16	1.31																						
CSE	UC	1.23	2.37	1.07	1.12	1.21																						
	TC	1.23	2.37	1.07	1.12	1.21																						
	MD	1.18	1.98	1.15	1.16	1.15	2.08	2.08	1.18	1.20	1.16	1.20	1.16	1.28	2.15	1.19	1.23	1.18	1.32	2.20	1.21	1.32	2.20	1.21	1.32	1.19	1.19	
CSB	UD	1.24	2.29	1.18	1.20	1.23	1.40	2.94	1.24	1.29	1.35	1.29	1.35	1.50	3.33	1.28	1.35	1.43	1.60	3.72	1.32	1.49	1.60	3.72	1.32	1.49	1.50	
	UC	1.17	1.85	1.14	1.15	1.12	1.23	1.91	1.17	1.18	1.13	1.18	1.13	1.26	1.97	1.18	1.21	1.15	1.31	2.04	1.21	1.30	1.31	2.04	1.21	1.30	1.16	
	TC	1.17	1.85	1.14	1.15	1.13	1.23	1.91	1.17	1.18	1.13	1.18	1.13	1.26	1.97	1.18	1.20	1.14	1.31	2.04	1.20	1.29	1.31	2.04	1.20	1.29	1.15	
PL2	MD	1.30	4.01	1.20	1.25	1.64	1.30	3.93	1.20	1.25	1.62	1.32	1.22	1.35	4.00	1.22	1.27	1.61	1.39	4.04	1.23	1.36	1.39	4.04	1.23	1.36	1.60	
	UD	1.37	4.57	1.23	1.29	1.73	1.46	5.64	1.27	1.35	1.88	1.46	1.88	1.57	6.33	1.31	1.40	1.94	1.67	6.99	1.34	1.53	1.67	6.99	1.34	1.53	2.02	
	UC	1.30	3.80	1.19	1.24	1.63	1.31	3.80	1.19	1.24	1.58	1.40	1.58	1.40	3.91	1.21	1.25	1.57	1.48	3.87	1.22	1.33	1.57	3.87	1.22	1.33	1.56	
CSE	TC	1.30	3.80	1.19	1.24	1.61	1.31	3.80	1.19	1.23	1.58	1.40	1.58	1.40	3.91	1.21	1.24	1.55	1.48	3.87	1.22	1.32	1.54	3.87	1.22	1.32	1.54	
	MD	1.39	2.03	1.17	1.24	1.10	1.56	2.46	1.22	1.32	1.22	1.32	1.22	1.67	2.74	1.24	1.36	1.27	1.76	3.11	1.27	1.49	1.76	3.11	1.27	1.49	1.34	
	UD	1.50	2.46	1.21	1.30	1.22	1.78	3.51	1.29	1.43	1.46	1.46	1.46	1.97	4.22	1.34	1.51	1.59	2.11	5.19	1.38	1.68	2.11	5.19	1.38	1.68	1.70	
PL3	UC	1.38	1.83	1.17	1.24	1.12	1.56	2.22	1.22	1.31	1.24	1.24	1.24	1.66	2.47	1.24	1.34	1.31	1.73	2.78	1.27	1.46	1.73	2.78	1.27	1.46	1.37	
	TC	1.38	1.83	1.16	1.22	1.09	1.56	2.22	1.21	1.28	1.20	1.28	1.20	1.66	2.47	1.23	1.32	1.25	1.73	2.78	1.25	1.44	1.73	2.78	1.25	1.44	1.32	
	MD	1.70	4.07	1.30	1.43	1.38	1.60	4.35	1.23	1.34	1.43	1.43	1.43	1.61	4.62	1.21	1.33	1.46	1.68	4.96	1.21	1.40	1.68	4.96	1.21	1.40	1.55	
CSE	UD	1.83	4.78	1.35	1.50	1.56	1.82	6.25	1.31	1.46	1.73	1.88	7.01	1.88	7.01	1.31	1.47	1.80	2.05	8.12	1.32	1.58	2.05	8.12	1.32	1.58	1.98	
	UC	1.73	3.82	1.34	1.42	1.38	1.59	3.90	1.26	1.34	1.39	1.60	4.14	1.60	4.14	1.24	1.32	1.39	1.62	4.38	1.23	1.40	1.62	4.38	1.23	1.40	1.49	
	TC	1.73	3.82	1.32	1.40	1.40	1.59	3.90	1.25	1.31	1.35	1.60	4.14	1.60	4.14	1.22	1.30	1.36	1.62	4.38	1.22	1.35	1.62	4.38	1.22	1.35	1.46	
PL4	MD	1.57	2.25	0.87	1.08	1.09	1.67	3.06	0.90	1.11	1.14	1.76	3.33	3.33	0.91	1.14	1.20	1.82	3.97	0.93	1.22	1.28	1.82	3.97	0.93	1.22	1.28	
	UD	1.68	3.10	0.95	1.18	1.36	1.96	3.99	1.00	1.26	1.49	2.06	4.77	4.77	1.03	1.29	1.63	2.15	6.18	1.03	1.41	2.15	6.18	1.03	1.41	1.78		
	UC	1.50	2.23	0.88	1.02	1.08	1.58	2.66	0.91	1.04	1.12	1.66	3.10	3.10	0.93	1.06	1.18	1.75	3.48	0.93	1.15	1.75	3.48	0.93	1.15	1.26		
CSE	TC	1.50	2.23	0.85	0.95	0.95	1.59	2.66	0.88	1.00	0.99	1.67	3.10	3.10	0.90	1.02	1.07	1.74	3.48	0.91	1.12	1.74	3.48	0.91	1.12	1.14		
	MD	2.52	4.71	1.14	1.57	1.68	2.01	4.52	1.02	1.33	1.69	1.99	4.66	4.66	0.99	1.26	1.76	2.01	5.11	0.97	1.30	2.01	5.11	0.97	1.30	1.77		
	UD	2.76	5.91	1.32	1.72	2.09	2.35	6.06	1.19	1.58	1.98	2.28	6.68	6.68	1.16	1.57	2.23	2.38	7.62	1.15	1.51	2.38	7.62	1.15	1.51	2.32		
CSE	UC	2.20	4.14	1.20	1.33	1.59	1.94	3.63	1.09	1.16	1.66	1.94	3.67	3.67	1.05	1.14	1.71	1.94	4.12	1.05	1.20	1.94	4.12	1.05	1.20	1.75		
	TC	2.20	4.14	1.11	1.21	1.46	1.94	3.63	1.00	1.08	1.58	1.94	3.67	3.67	0.99	1.06	1.66	1.94	4.12	0.98	1.11	1.94	4.12	0.98	1.11	1.69		

PL1, ..., PL4 = length of the central pier, as described in Section 3.2
 WBH1, ..., WBH4 = height of the window bank as described in Section 3.2
 CSB = Calcium Silicate Brick masonry; CSE = Calcium Silicate Element masonry
 RC = Reinforced concrete floor; T = timber floor; C = continuous façade
 MD = modal proportional distributed loads; UD = mass proportional distributed loads; UC = mass proportional concentrated loads; TC = triangular concentrated loads

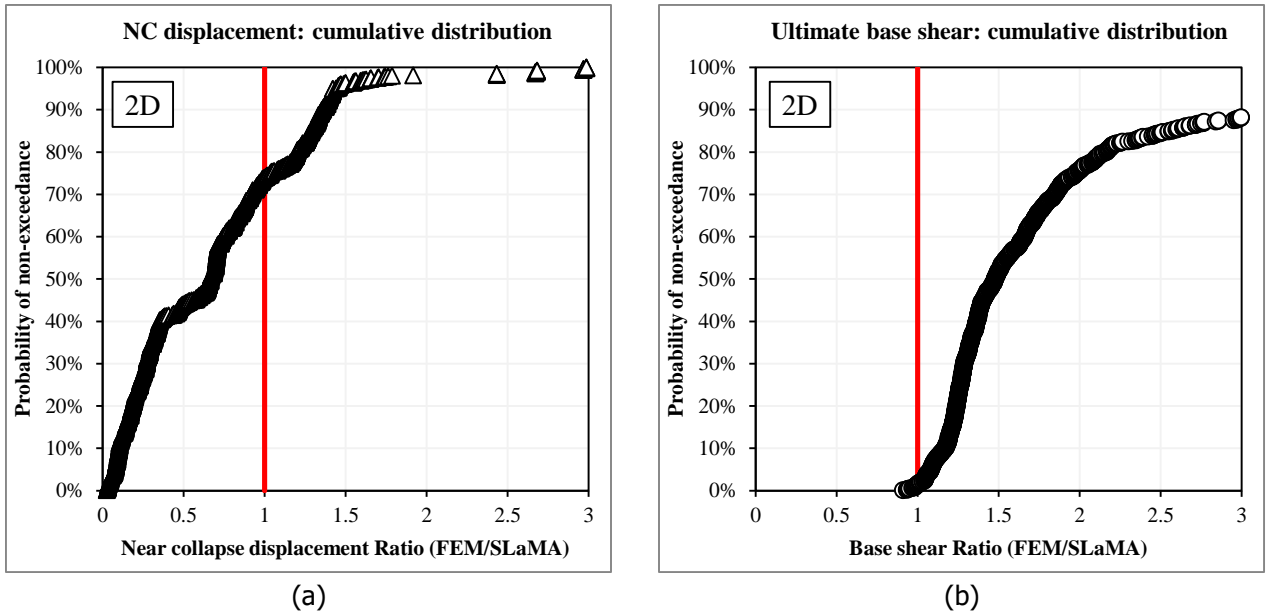


Figure 16. Cumulative distribution functions for the ratio computed for the results of 2D NLFEA and SLaMA analyses: near collapse displacement (a) and ultimate base shear (b).

Figure 17 and Figure 18 are used to analyse the influence of different parameters on the ratio between the values of Near Collapse displacement and the Ultimate Base Shear computed for the 2D NLFEA and SLaMA analyses, respectively. Figure 17 makes use of radar charts that highlight the parameters for which larger differences between the two computational methods are observed. Figure 18 shows the cumulative distribution functions computed for different groups of analyses: different materials (a); no. of storeys (b); different floor type at the attic level (c); structural continuity of the façade (d); length of the pier (e). It should be noted that smaller differences are found between the NLFEA and SLaMA analyses when the curves are steeper and closer to the value one.

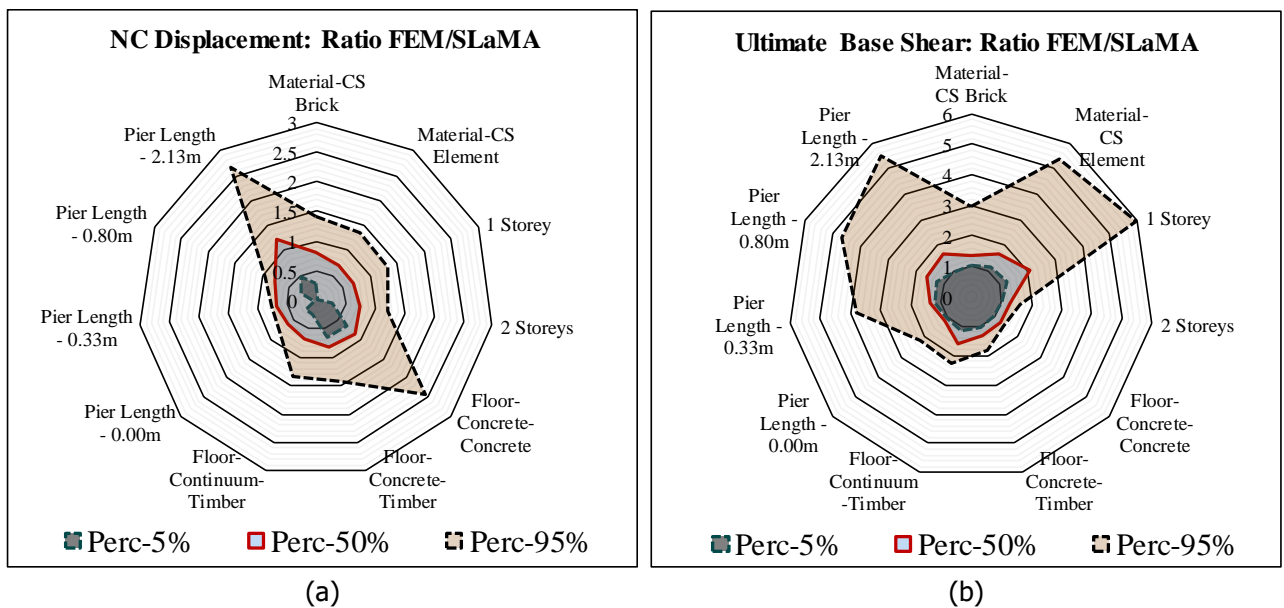


Figure 17. Influence of the different parameters on the ratio NLFEA/SLaMA of 2D analyses for the Near Collapse displacement (a) and the Ultimate Base Shear (b).

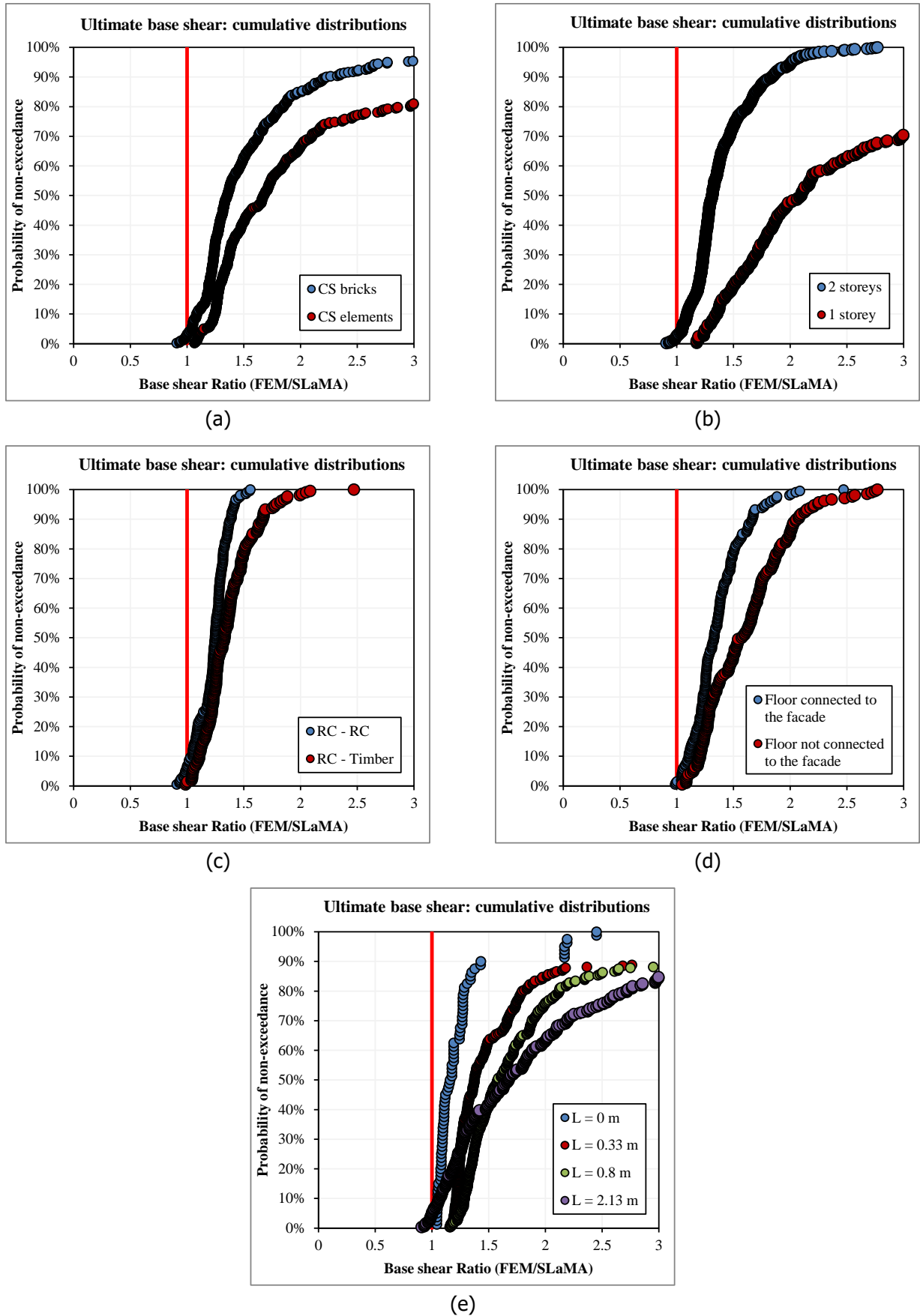


Figure 18. Cumulative distribution functions for the ratio computed for the results of NLFEA and SLaMA analyses: near collapse displacement (a) and ultimate base shear (b).

The figures show clearly that a larger difference between the ultimate base shear computed with NLFEA and SLaMA analyses is obtained: (1) for single storey buildings; (2) with CS element masonry; (3) when the façade is not structurally connected to the RC slab at the first floor level; (4) when long, squat piers are present in the façade (i.e. when other failure mechanisms than flexure are expected). When these results are compared with those obtained with the 3D modelling of the whole building, large ratios are obtained also for the analyses corresponding to points (2-4) of the list presented above (#04, #05, #07, #11, #12, #14). The largest ratio is in fact obtained for case #04, in the negative direction (with a ratio equal to 4.81, Table 6), which presents a geometry with a long, squat pier on both the façades, resulting in a behaviour mainly governed by the shear capacity of that pier. This capacity appears to be underestimated with the SLaMA method when compared to the results of the corresponding NLFEA. It is also important to note that no significant difference is found in the 3D analyses between the curves of the one- and two-storey buildings.

In conclusion, the 2D analyses mainly confirm the trends and values obtained for the 3D analyses. The larger number of cases considered allows also to define the parameters for which larger differences between the NLFEA and SLaMA analyses are found, as regards the ultimate base shear. These cases are:

- with the use of CS elements;
- when the façade is not structurally connected to the RC slab at the first floor level;
- when the façade is characterised by the presence of at least one long, squat wall with an aspect ratio larger than one.

6 Conclusions

This report presents the results of a study that aims to compare the outcomes of nonlinear finite element analyses (NLFEA) and mechanism based analyses when nonlinear pushover analyses are performed in accordance with the recommendations provided in NPR 9998 [1]. The study focuses on a specific group of buildings: the terraced houses. This group of buildings is characterized by a resisting system composed of unreinforced masonry (URM) walls; large openings and vertical irregularities on the façades, and solid walls in the transversal direction; cavity walls with calcium silicate (CS) masonry commonly used for the loadbearing walls, one or two storeys up to the attic level. Building EUC-BUILD-6, which was tested in dynamic conditions on a shake table at the laboratory of EUCENTRE (Pavia, Italy), was taken as reference building for a terraced house unit.

A large number of variations of the case study have been performed: 48 3D analyses of the complete building, and 1040 2D analyses of a single façade of the building. The most of variations focused on (i) the layout of the façades, (ii) the masonry type used, (iii) the floor type at attic level and (iv) the and the floor-façade connection.

The analysis of the results obtained for NLFEA and SLaMA analyses performed suggests that:

1. NLFEA and SLaMA identify the same failure mechanism for this typology of buildings in 94% of the 3D analyses. The failure mechanism is usually governed by the rocking of the piers at the ground storey. Specifically a governing rocking mechanism was predicted in the 3D analyses by both NLFEA and SLaMA for 85% of the cases. In 9% both predicted shear failure mechanism. In the remaining 6% of cases no clear governing mechanism could be identified in the NLFEA predicted predominant shear failure and while SLaMA predicted flexural failure.
2. Similar values of the initial stiffness of the building and of the yielding displacement in the equivalent bilinear curve are obtained on average for the two computational methods (average factor: 1.23).
3. The near collapse displacement capacity of the building is often limited in the NLFEA by the global drift limit at inter-storey level (1.5% for ductile mechanisms). This value is close to the average near collapse displacement computed for the SLaMA analyses, which is mainly governed by the flexural displacement capacity of the single piers. This results confirm that the value proposed in Table G.2 of NPR 9998:2018 [1] for the global drift limit in case of ductile mechanisms is in accordance to the displacement capacity of the building computed considering the drift limits of the single walls.
4. As regards the ultimate base shear, large differences between the results obtained according to the two methods are found: when 3D analyses are considered, the NLFEA return a base shear capacity on average more than 2.5 times higher than that computed according to the SLaMA method, and 1.5 times higher for more than the 95% of the cases analysed.
5. Even larger difference between the ultimate base shear computed with NLFEA and SLaMA is obtained in the following three cases: with CS elements; when the façade is not structurally connected to the RC floor at the first floor level; when long, squat piers are present in the façade (i.e. when other failure mechanisms than flexure are expected). For the twelve 3D analyses where the buildings present one of these characteristics, the ratio between the base shear computed according to NLFEA and SLaMA is always larger than 2.25.

Based on the conclusions stated above, when the SLaMA method is used to define the capacity of a building having characteristics in line with those considered in this study (reported in Sections 2 and 3, as well as in [4]), it is suggested to apply no correction factor to the initial stiffness and the ultimate displacement capacity.

A factor can be applied to increase the value of the ultimate base shear computed with the SLaMA method. In general, the factor can be taken equal to 1.5, because this provides conservative results in the 95% of cases (with respect to the corresponding NLFEA), as shown in Figure 19a. The correction factor can be

increased up to the value 2 when a building presents one of the three following characteristics: (i) use of CS elements, (ii) structural continuity of the loadbearing façade (i.e. the RC floor is not connected to the inner leaf of the façade, except for anchors that can only prevent the out-of-plane failure), (iii) presence of long, squat piers with an aspect ratio larger than one. In fact, the suggested value 2 is smaller than the minimum ratio computed between the base shear computed according to NLFEA and SLaMA for the twelve 3D simulations performed on buildings with such characteristics (Figure 19b).

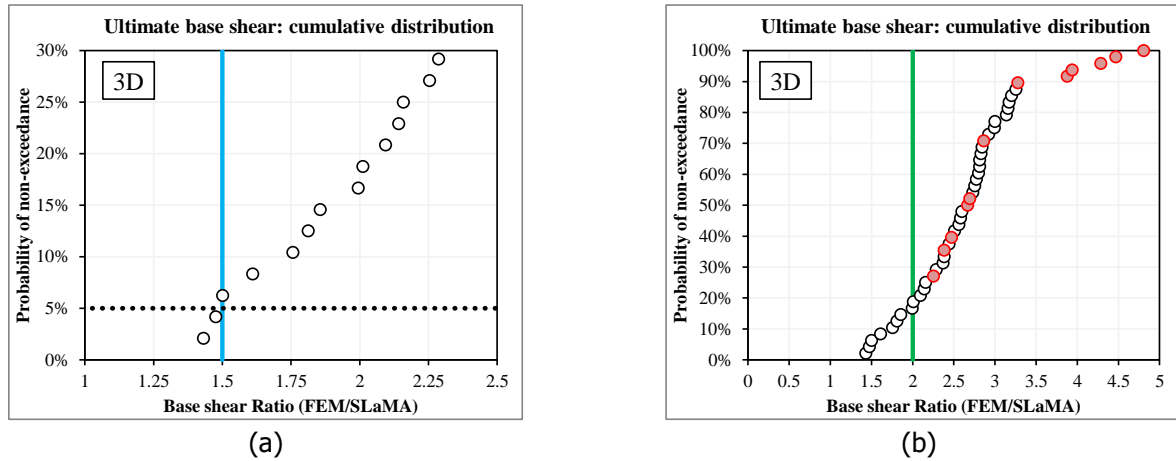


Figure 19. Cumulative distribution functions for the ratio between the ultimate base shear computed for the results of 3D NLFEA and SLaMA analyses: detail for low probability of non-exceedance (a), and for the analyses with CS elements, structural continuity of the loadbearing façade and long piers, highlighted by red markers (b).

References

- [1] NEN, Nederlands Normalisatie Instituut (2018). NPR 9998:2018 nl. Beoordeling van de constructieve veiligheid van een gebouw bij nieuwbouw, verbouw en afkeuren - Geïnduceerde aardbevingen - Grondslagen, belastingen en weerstanden. Delft, the Netherlands (in Dutch)
- [2] Messali, F., Rots, J.G. (2018). EUC-BUILD-6: post-test refined predictions (TU Delft – DIANA 10.2). TU Delft Report, 28 October 2018
- [3] Messali, F., Rots, J.G., Longo, M. (2018). Prediction of the peak base shear capacity of seven experiments on full-scale URM structures: comparison between different methods. Memorandum TU Delft, TUD_NPR9998_Memo_08-Draft01, 27 September 2018
- [4] Messali, F. (2019). Cross-validation and calibration of simplified methods for different building typologies. TU Delft Proposal, Final version, 24 September 2019
- [5] Tünnissen, J. (2019). TN 18 – Clustering. Memorandum CVW, 21 March 2019
- [6] Tünnissen, J. (2019). TN 20 – Selectiecriteria Prio-clusters. Memorandum CVW, 25 September 2019
- [7] Miglietta, M., Mazzella, L., Grottoli, L., Guerrini, G., Graziotti, F. (2019). Full-scale shaking table test on a Dutch URM cavity-wall terraced-house end unit – EUC-BUILD-6. EUCENTRE report EUC160/2018U. Version 2.0, 07 March 2019
- [8] Messali, F., Longo, M. (2019). Validation of a mechanism-based method against FEM for NLPO analyses of a URM terraced unit. Delft University of Technology. Report number 01, Version 01, 17 October 2019
- [9] Esposito, R., Terwel, K.C., Ravenshorst, G.J.P., Schipper, H.R., Messali, F., Rots, J.G. (2017). Cyclic pushover test on an unreinforced masonry structure resembling a typical Dutch terraced house. Proceedings of the 16th World Conference Earthquake Engineering, Santiago, Chile
- [10] BiCL NL (2018). Seismic Assessment Criteria (Basis of Assessment). Revision 0.1, 23 January 2018
- [11] Moon, F.L., Yi, T., Leon, R.T., Kahn, L.F. (2006) Recommendations for Seismic Evaluation and Retrofit of Low-Rise URM Structures, *Journal of Structural Engineering*, 132(5), 663-672